CHAPTER IV

EXPERIMENTAL RESULTS

The excitation functions of twenty three reactions of the types (α,xn); (α,pxn) and (α,αxn) are measured up to 50 MeV using stacked foil activation technique and high resolution HPGe detector (2.0 keV FWHM for 1332 keV photons of ^{60}Co).These reactions were previously measured with poor resolution scintillation detector as well as with Ge detector . There are large mutual discrepancies in the cross section values for the same reactions even in the Ge detector measurements. In this context the present investigation was undertaken with two aims

(i) to make careful and systematic experimental study of the individual excitation functions and

(ii) to compare the measured excitation functions of the reactions with hybrid model of Blann (ALICE/90).

In the following paragraphs, the salient features of each reaction are mentioned together with the comparison of the present and previous results, wherever available.

IV.1 Alpha Particle Induced Reactions in the Target Element Gold :

Gold is a typical heavy element which is mono isotopic (100%) and obtainable in its purest form (99.99%). It has very good metallic properties by which it is possible to obtain uniform thin foils suitable for the stacked foil activation technique. It is interesting to measure the total reaction cross section in such a heavy element where the contributions due to a fission competition are remarkably high. The following reactions have been studied in the present work with this target : $^{197}Au(\alpha,n)$, $^{197}Au(\alpha,2n)$, $^{197}Au(\alpha,3n)$, $^{197}Au(\alpha,2pn)$ and $^{197}Au(\alpha,\alpha n)$ /1/.

While there is only one group, Lanzafame and Blann /2/ who measured all the five reactions using a Ge detector earlier in 1970, other investigators, Kurz et al /3/, Capurro et al /4/ and Bhardwaj et al /5/ had confined only to the (α,xn) ; x=1-3 reactions, whose cross sections are generally large compared to those of (α,pxn) and (α,αxn) reactions , involving the emission of charged particles.

The salient features of the reactions studied are presented below:

IV.1.1 Excitation function of the $^{197}Au(\alpha,n)^{200}Tl$ reaction :

In general single neutron emitting reactions of the type (α,n) are interesting in several ways: firstly, the initial part of their excitation function defines the initial rise of the total reaction cross section for low energies. Secondly, direct reaction contributions are more likely in single nucleon emission reaction as compared to those involving many nucleons. Thirdly, preequilibrium mechanism is expected to play a major role at energies exceeding a few tens of MeV.

This reaction previously measured by Lanzafame and Blann (1970), Kurz et al (1971), Capurro et al (1985) and Bhardwaj et al (1986), all using stacked foil activation technique. Lanzafame and Blann /2/ measured this reaction in the energy range 18-95 MeV using scintillation detector as well as Ge(Li) detector. The lower limit of uncertainty in their measurement was quoted as 20%.

Kurz et al /3/ studied this reaction upto 43 MeV employing a small volume (7 cm^3) Ge(Li) detector with a resolution of 4.2 keV for the 1170 keV γ-ray of ^{60}Co. The experimental error in the cross section was quoted to be less than 10%, but

it is not mentioned whether or not this includes the uncertainty in the monitor cross section used for the flux measurement.

Capurro et al /4/ measured the reaction upto 55 MeV using an intrinsic Germanium detector. The overall error in their measurement varied in the range 24 to 37 %. Bhardwaj et al /5/ measured this reaction upto 40 MeV using the HPGe detector with an error upto 17 % in the lower energy region. It can be seen from figure IV.1 that the four measurements however, do not agree with one another in the overlapping energy region. The measurements of Capurro et al are about a factor two smaller than the measurements of Lanzafame and Blann. Also the values of Capurro et al and Bhardwaj et al differ by more than 50 % around 30 MeV and the deviation is larger at higher energies.

In the present work, the residual nucleus ^{200}Tl was identified by its characteristic 368, 579 and 1206 keV gamma rays using a high resolution 120cc HPGe detector (~ 2 keV FWHM for 1332 keV photons of ^{60}Co). The product nucleus having half life 26.1 h and spin 2^-. A typical gamma ray spectrum and partial decay scheme are shown in figure IV.6 and IV.7(a) respectively. The cross sections were calculated using the prominent 368 keV gamma ray peak. The error in our measurement is less than 8% thereby showing not only an improved accuracy but also as evident from figure IV.1, a better shape of the excitation function compared to those of others.

IV.1.2 Excitation function of the ^{197}Au(α,2n)^{199}Tl reaction :

This reaction was also previously measured by the same four authors, Lanzafame and Blann (1970) , Kurz et al (1971), Capurro et al (1985) and Bhardwaj et al (1986) in the different energy range. The experimental procedure being the

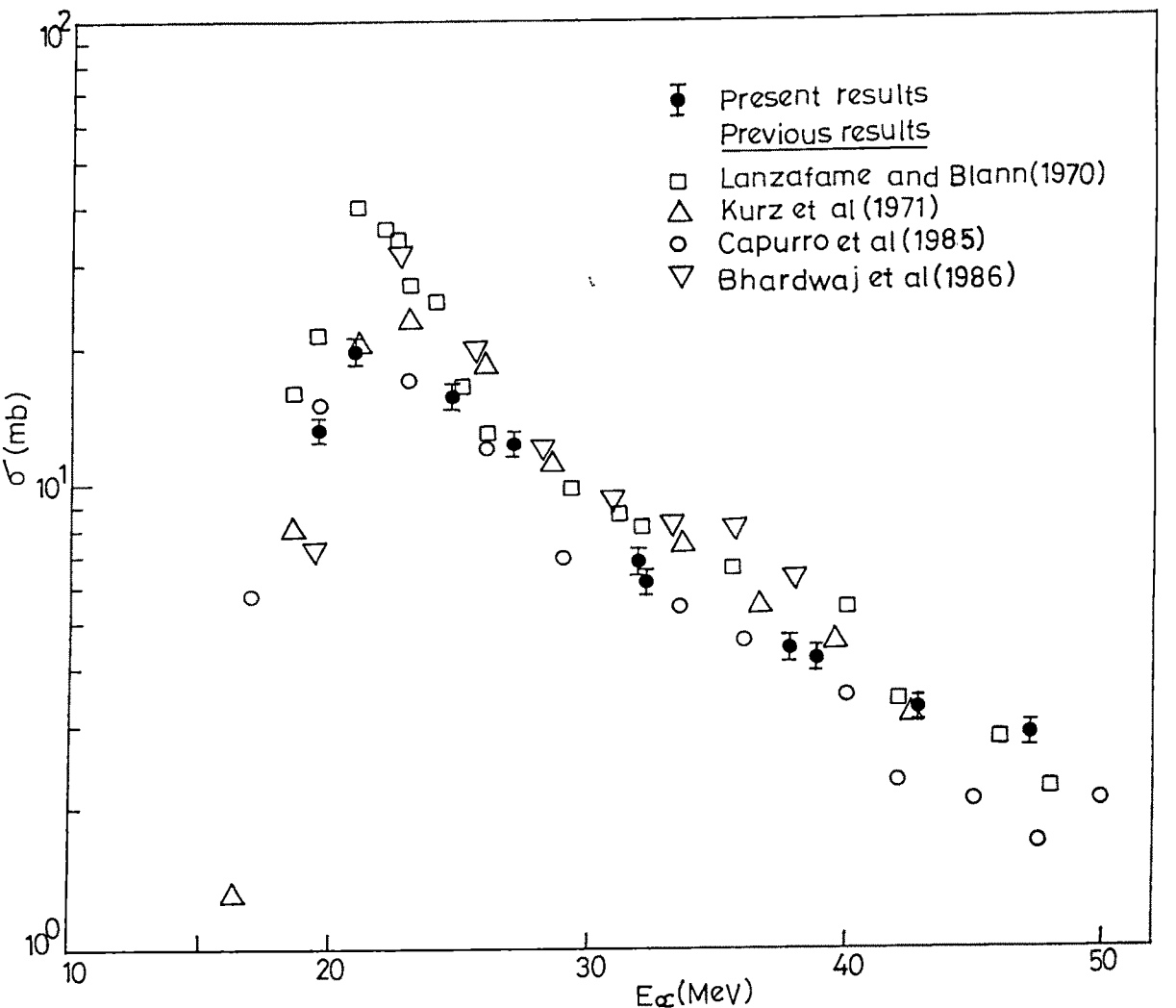

Fig.IV.1 EXCITATION FUNCTION OF $^{197}Au(\alpha,n)^{200}Tl$ REACTION

same as in the previous one. So far as the magnitude of the cross sections are concerned, there is a fairly good agreement among the results. However, the uncertainties in the measurement were stated to be 20% in the lower limit by Lanzafame and Blann , while those of Capurro et al vary from 13% to as high as 75% at some points. Kurz et al mentioned the uncertainty of about 10 %.

To improve the quality of data for this reaction, it is reinvestigated in the present work using a 120 cc HPGe detector having resolution 2 keV for 1332 keV photons of ^{60}Co. The residual nucleus ^{199}Tl having half life 7.42h and spin $1/2^{+}$, was identified by its characteristic 208, 247 and 455 keV gamma rays . A typical gamma ray spectrum and partial decay scheme are shown in figure IV.6 and IV.7(b) respectively. The cross sections were calculated using 455 keV gamma ray with an error less than 8% and gives better agreement with those of previous measurements as shown in figure IV.2. The calculation was also done with the other characteristic gamma rays in order to get a consistency check on the cross section measurements.

IV.1.3 Excitation function of the ^{197}Au(α,3n)^{198}Tl reaction :

This reaction has also been measured by four groups. The only difference is that Lanzafame and Blann /2/, who investigated this reaction had mentioned only an "estimated average fractional precision" of 6% in the cross section measurements , but did not give the overall error , because of the uncertainties in the available decay scheme data. Capurro et al /4/ mentioned estimated errors of 25-40 %.

In view of the clear need for re-investigation, this reaction was studied in the present work employing the accurate spectroscopic data and high resolution HPGe detector. The product nucleus ^{198}Tl having an isomeric state ^{198m}Tl (half life 1.87 h and spin 7^{+}) which decays to the ground state ^{198g}Tl(half life 5.3h and spin 2^{-})

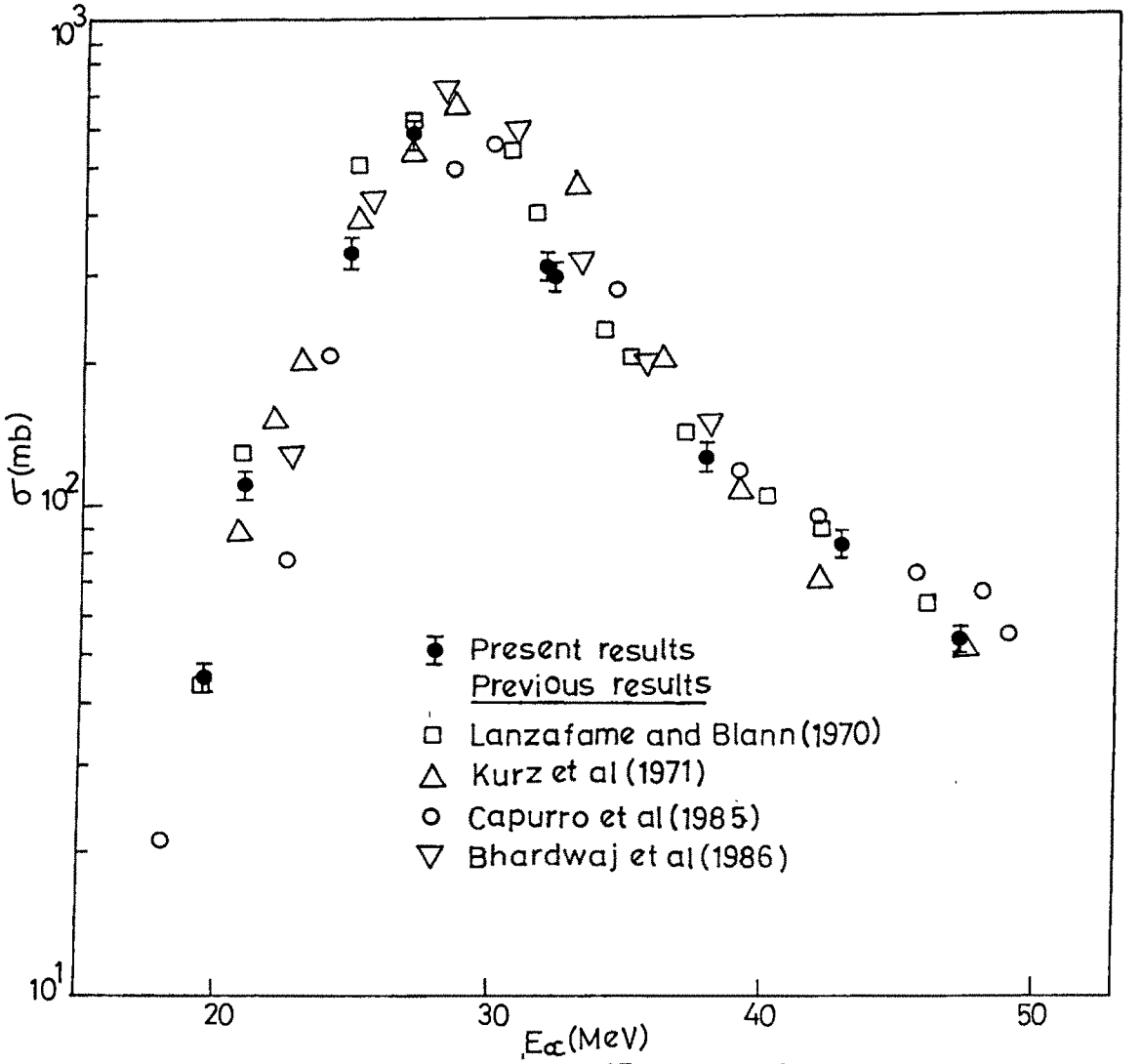

Fig.IV.2 EXCITATION FUNCTION OF $^{197}Au(\alpha,2n)^{199}Tl$ REACTION

through an isomeric transition. Since the data collection was performed after the complete decay of the metastable state to the ground state, the sum of the cross section for the isomeric and ground states ,was determined in the present work.

The product nucleus ^{198g}Tl was identified by its characteristic 637 and 676 keV gamma rays .A typical gamma ray spectrum and partial decay scheme are shown in figure IV.6 and IV.7(c) respectively. The cross sections were calculated using the 676 keV gamma ray as shown in figure IV.3. It can be seen from figure that present results, while generally agreeing with previous one, serve to limit the errors on the cross section to the minimum so as to enable a meaningful comparison with theoretical predictions to be made in the next chapter.

IV.1.4 Excitation function of the ^{197}Au(α,2pn)^{198} Au reaction :

The study of this reaction is interesting from the view point of large Coulomb barrier offered by a heavy nucleus like gold to the emission of charged particles. This reaction was measured only by Lanzafame and Blann /2/ with an overall error of 20%. The residual nucleus ^{198}Au has an isomeric state ^{198m}Au having half life 2.3 d and spin 12$^-$ decaying to the ground state ^{198g}Au having half life 2.69 d and spin 2$^-$ through isomeric transition. A typical gamma ray spectrum and partial decay scheme are shown in figure IV.6 and IV.7(d) respectively. It is not clear from the paper of Lanzafame and Blann whether the reported cross section was the total or merely ground state cross section. In the present work we have measured ground state cross section using 412 keV gamma ray as shown in figure IV.4.

It can be seen from figure, that the shape of the excitation function is completely different from the general shape of (α,xn) excitation functions . The broad maximum at low energies due to the compound nucleus mechanism is

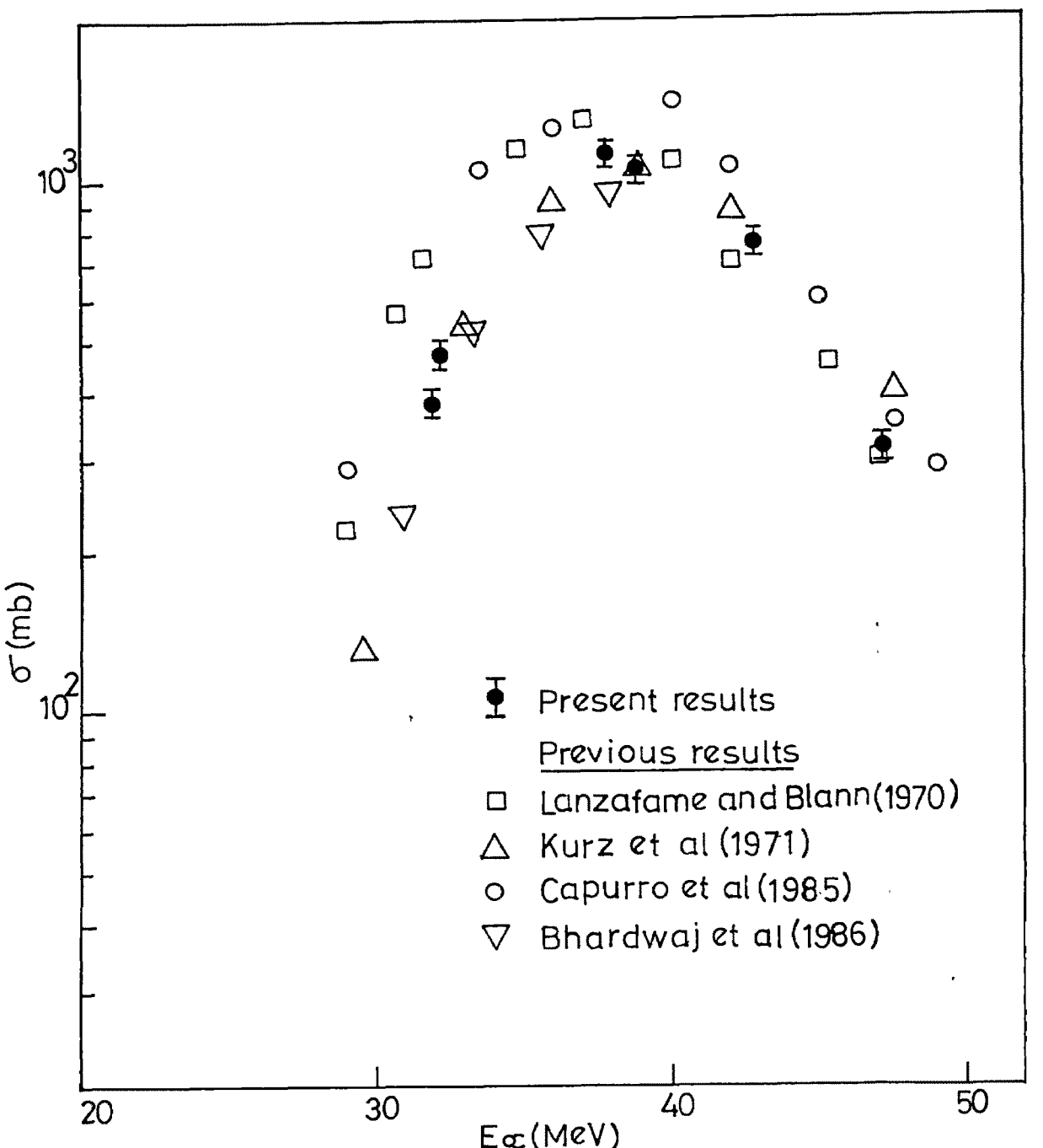

Fig.IV.3 EXCITATION FUNCTION OF $^{197}Au(\alpha,3n)^{198}Tl$ REACTION

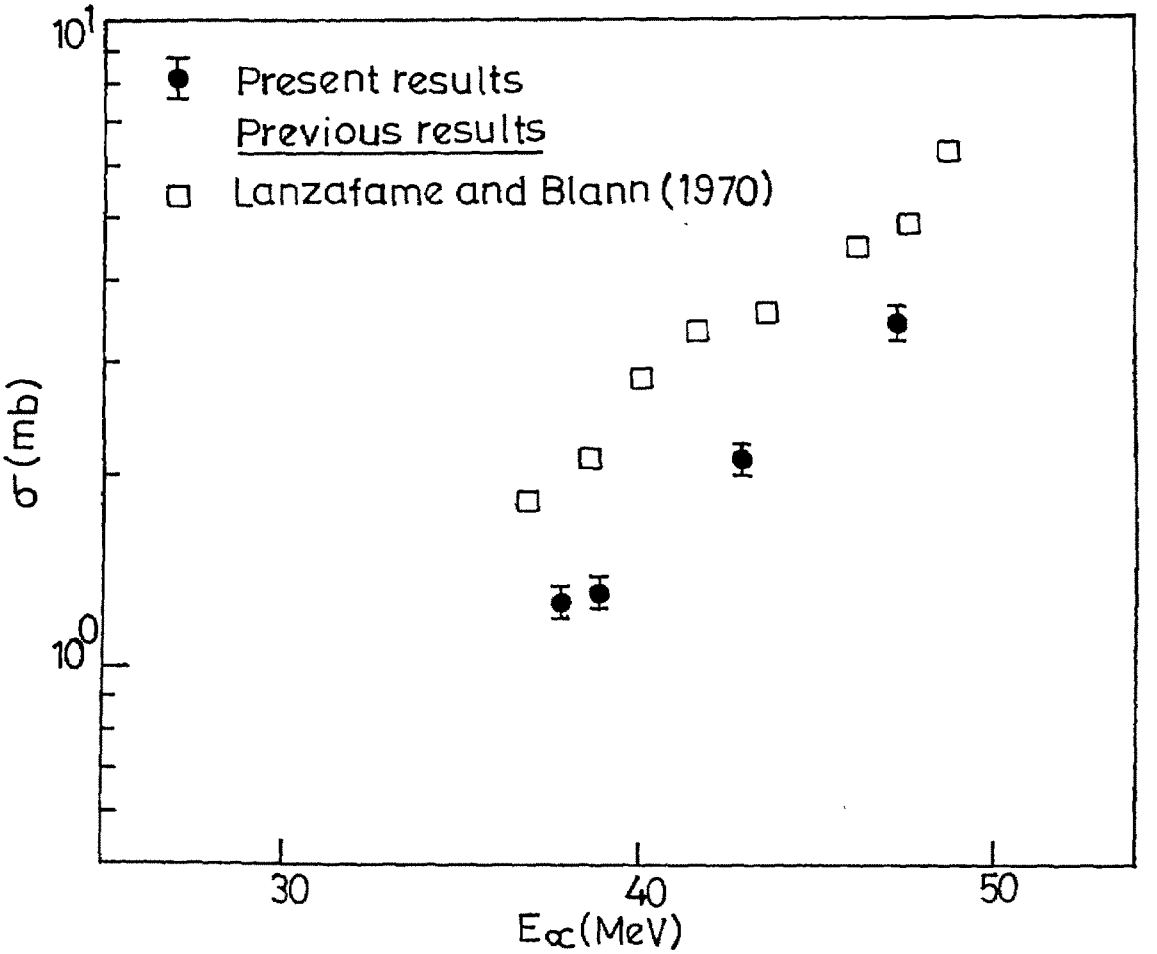

Fig.IV.4 EXCITATION FUNCTION OF $^{197}Au(\alpha,2pn)^{198}Au$ REACTION

conspicuously absent. This can be understood as being due to the strong inhibition of low energy protons, owing to the large Coulomb barrier offered by the compound nucleus to the evaporation of charged particles from it.

IV.1.5 Excitation function of the $^{197}Au(\alpha,\alpha n)^{196}Au$ reaction :

The study of $(\alpha,\alpha n)$ reaction on a heavy target element is difficult and interesting at the same time . It has in general low cross sections due to alpha particle emission so that their characteristic gamma ray photo peaks are marked by the compton background due to much stronger gamma rays coming from other reactions such as (α,xn) on the same target nucleus.

The interest in the study of $(\alpha,\alpha xn)$ reactions is centered around the mechanism of alpha particle emission. As discussed in chapter II, the basic assumption such as the existence of preformed alpha particles in nuclei and the ideas of coalescence models have to be tested against detailed experimental studies on $(\alpha,\alpha xn)$ type of reactions.

This reaction was earlier studied by Lanzafame and Blann /2/ with a lower limit of accuracy 15%. The product nucleus ^{196}Au occurs in two isomeric states, with half lives of 8.2s (^{196m}Au) and 9.7 h (^{196g}Au). Allowing time for the former to decay to the later, the sum cross section is usually measured following the 9.7 h ground state activity. The residual nucleus was identified by its characteristic 333 and 356 keV gamma rays. A typical gamma ray spectrum and partial decay scheme are shown in figure IV.6 and IV.7(e) respectively. The cross sections were measured

using 356 keV gamma ray shown in figure IV.5 together with the results of Lanzafame and Blann. It can be seen from figure that there is a satisfactory agreement between present and previous result.

A complete summary of the results obtained in the present experimental study is given in table IV.1.

IV. 2 Alpha Particle Induced Reactions in the Target Element Antimony :

This medium weight element in its natural form has two odd mass stable isotopes of abundances 57.3% (^{121}Sb) and 42.7% (^{123}Sb). Enrichment of antimony is not very difficult but the quantity of enriched isotope material required for the stacked foil technique is un economical and rarely used.

However, when a natural target is used in reaction studies, more than one isotope may contribute to the production of a given product nucleus through different reaction channels, for example, ^{121}Sb(α,n) and ^{123}Sb(α,3n) reactions leading to the same residual nucleus ^{124}I . In such cases the measured cross section, as explained in the chapter III.3.5, is the weighted average over the two reaction channels and can be easily interpreted taking into account the differences in the threshold energies and their relative predominance in a given energy range. The two contributions can therefore be separated out pretty accurately using either the known theoretical ratio of cross sections or by subtracting the contribution of one of the reactions measured with an enriched isotopes /6/. Efforts were made to separate the individual contributions of the reactions: ^{124}I is formed in ^{121}Sb(α,n) and ^{123}Sb(α,3n); ^{123}I is formed in ^{121}Sb(α , n) and ^{123}Sb(α,4n); ^{120}Sb is formed in

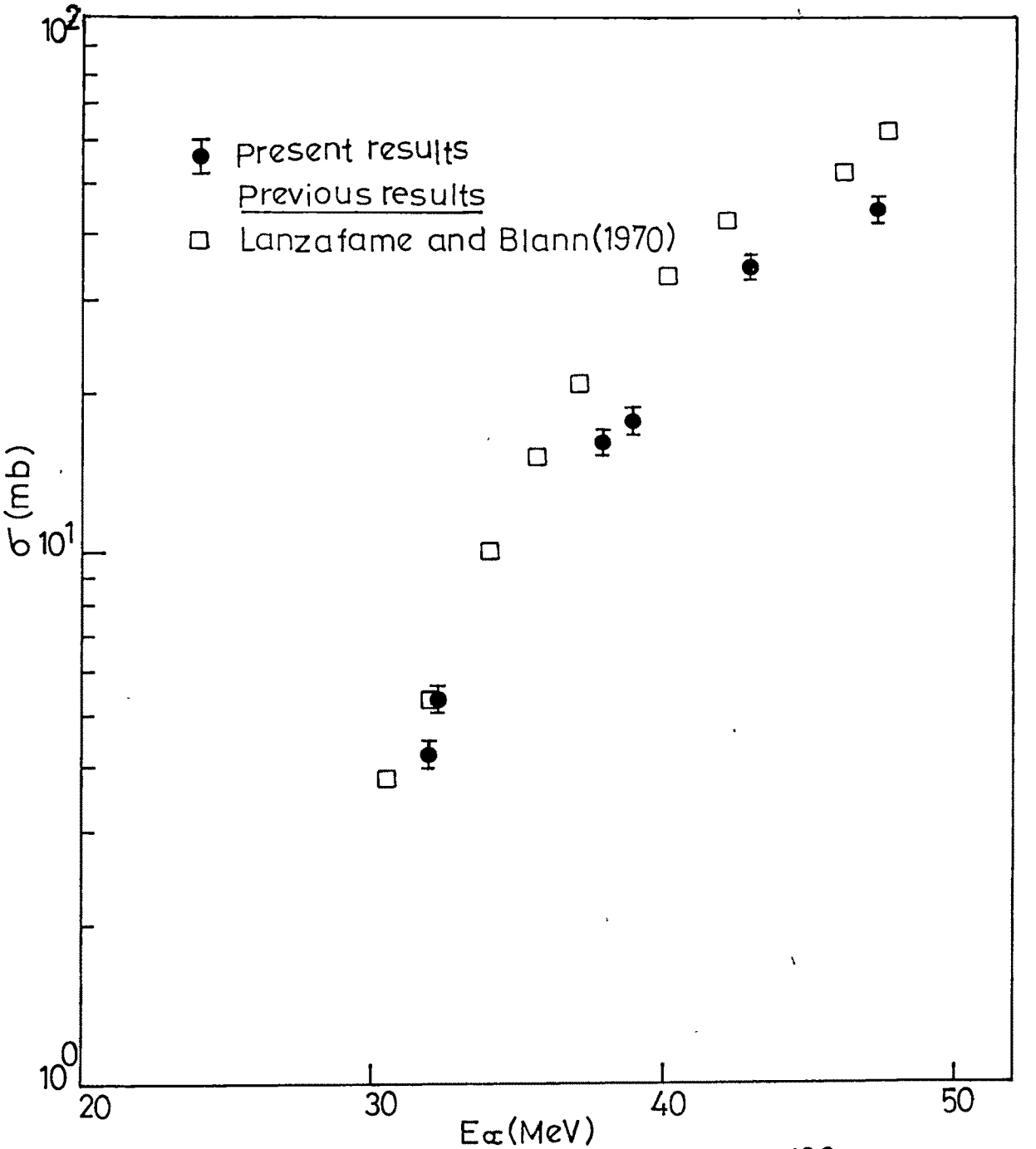

Fig.IV.5 EXCITATION FUNCTION OF $^{197}Au(\alpha,\alpha n)^{196}Au$ REACTION

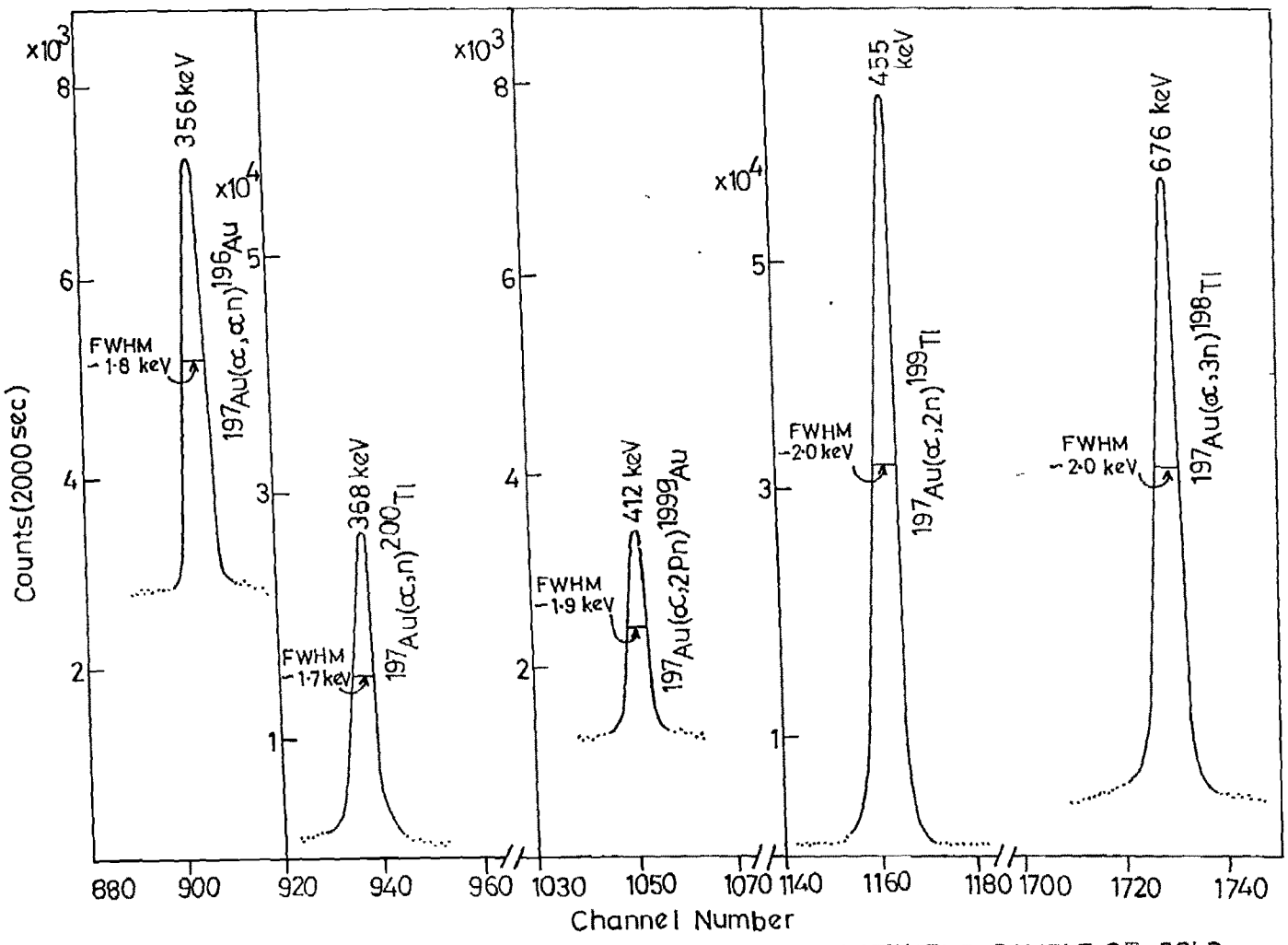

Fig.IV.6 A TYPICAL GAMMA RAY SPECTRUM OF ACTIVATED SAMPLE OF GOLD

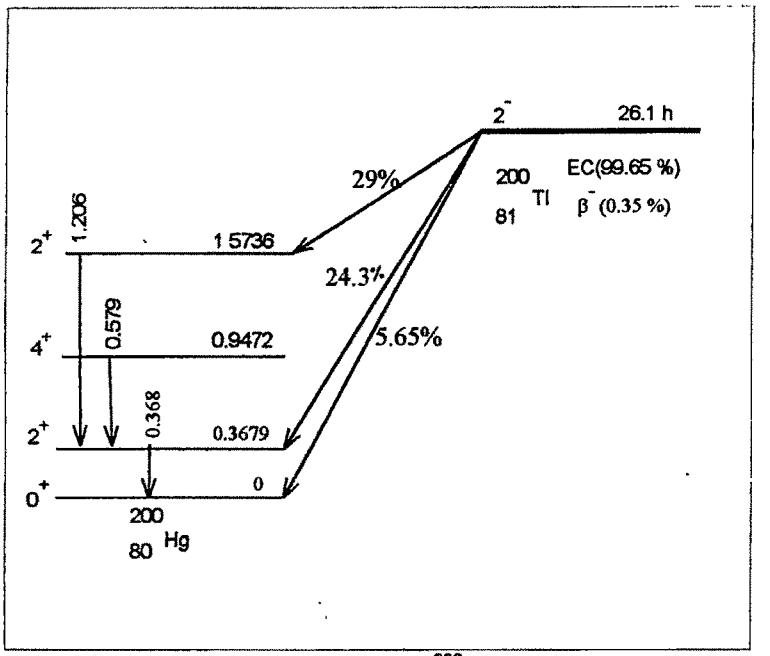

Fig.IV.7(a) Partial decay scheme of ^{200} Tl

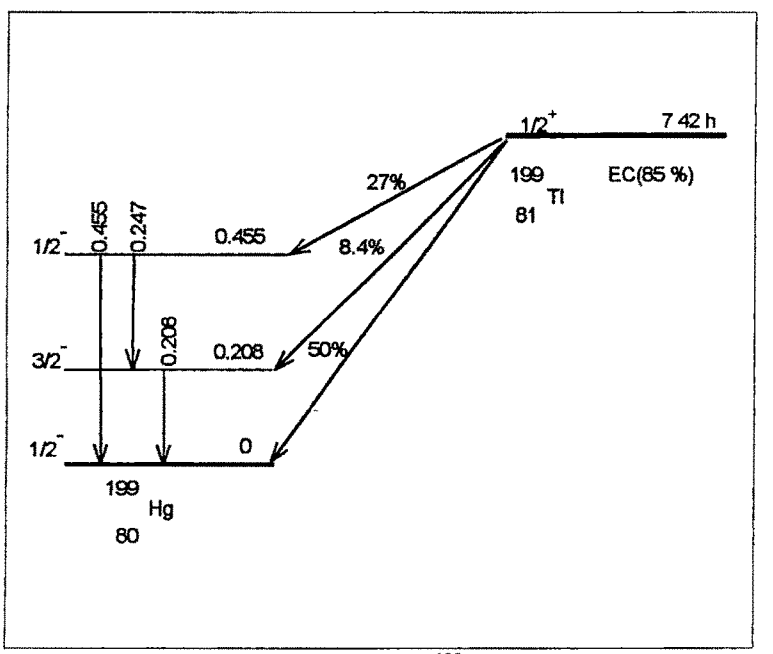

Fig.IV.7(b) Partial decay scheme of ^{199} Tl

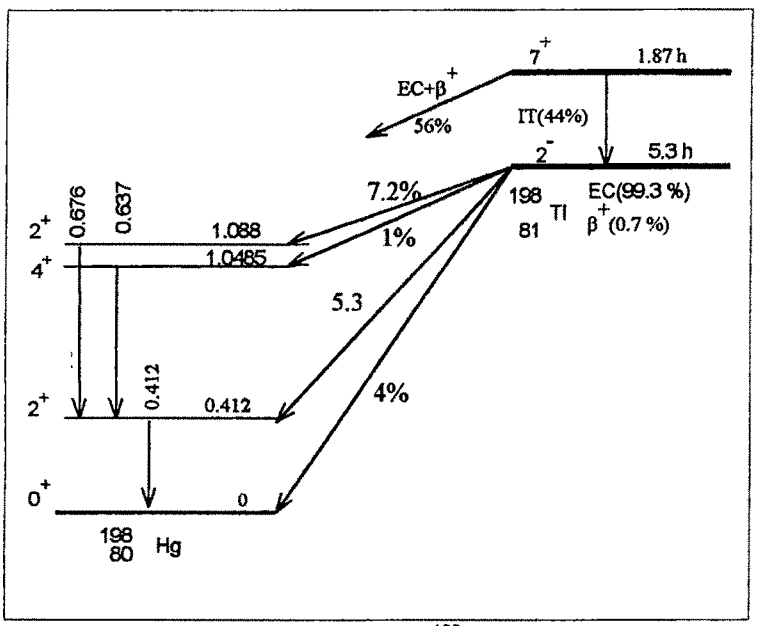

Fig.IV.7(c) Partial decay scheme of ^{198}Tl

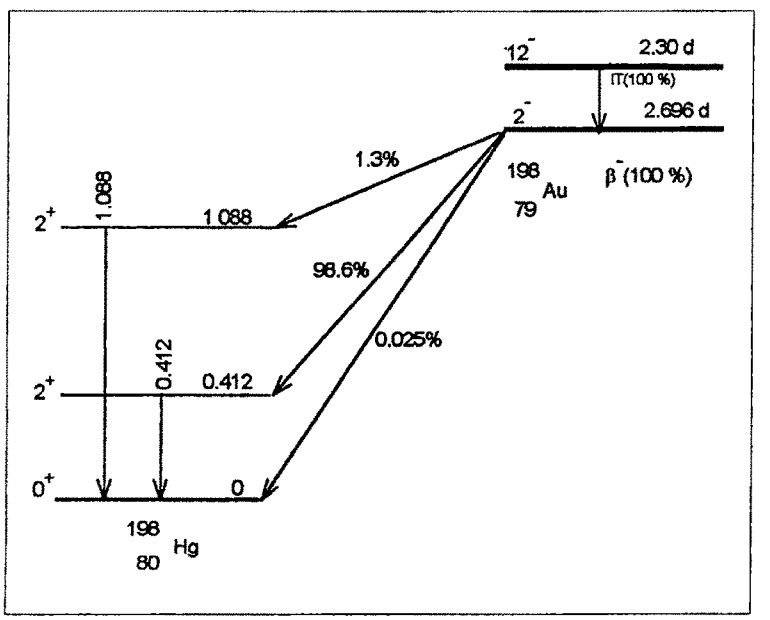

Fig.IV.7(d) Partial decay scheme of ^{198}Au

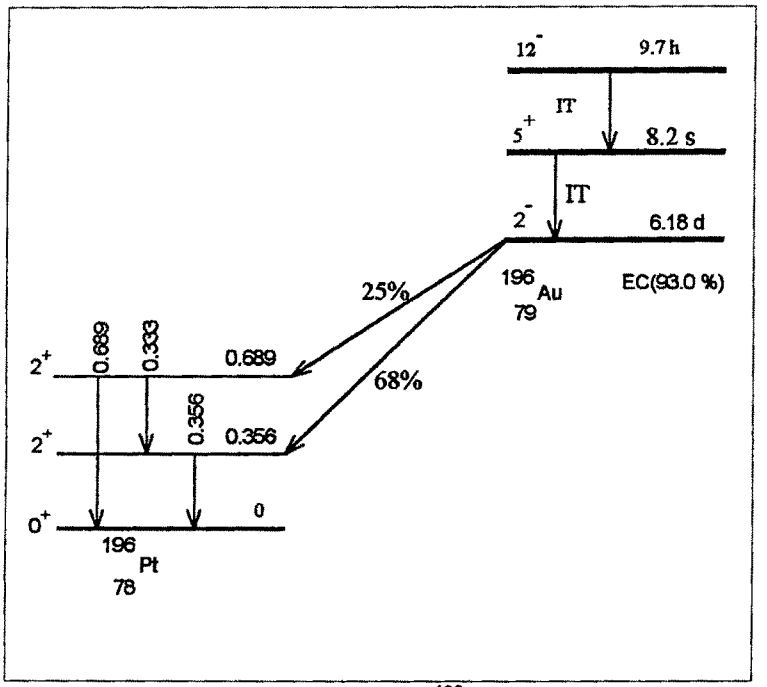

Fig.IV.7(e) Partial decay scheme of ^{196}Au

Table IV.1 Cross sections of the α-induced reaction on ^{197}Au measured in the present work.

Reaction	**^{197}Au(α,n)**	**^{197}Au(α,2n)**	**^{197}Au(α,3n)**	**^{197}Au(α,2pn)**	**^{197}Au(α,αn)**
Product nucleus	**^{200}Tl**	**^{199}Tl**	**^{198}Tl**	**^{198}Au**	**^{196}Au**
Threshold Energy (MeV)	9.93	18.16	26.40	24.26	8.16
E_α (MeV)	**σ(mb)**	**σ(mb)**	**σ(mb)**	**σ(mb)**	**σ(mb)**
19.5	13.2±1.5	044.8±05.4			
20.9	19.5±2.2	110.0±13.3			
24.7	15.8±1.8	332.0±40.1			
27.0	12.3±1.4	580.0±70.1			
31.9	06.8±0.8	310.0±37.7	0380.0±047.4		04.18±0.5
32.2	06.1±0.7	297.0±35.9	0470.0±058.6		05.33±0.6
37.8	04.4±0.5	125.0±15.1	1110.0±138.5	1.25±0.15	16.20±1.8
38.8	04.2±0.5	110.0±13.3	1050.0±131.0	1.30±0.15	17.40±1.9
42.8	03.3±0.4	082.4±09.9	0760.0±094.8	2.10±0.25	34.20±3.8
47.2	02.9±0.3	053.7±06.5	0315.0±039.3	3.40±0.40	43.50±4.9

$^{121}Sb(\alpha,\alpha n)$ and $^{123}Sb(\alpha,\alpha 3n)$ reaction respectively, using theoretical excitation function in the eqns. 11 & 12 of chapter III.3.5.. The following reactions have been studied in this element $^{121}Sb[(\alpha,n)$, $(\alpha,2n)$, $(\alpha,4n)$, $(\alpha,p3n)$, $(\alpha,\alpha n)]$ and $^{123}Sb[(\alpha,3n),(\alpha,4n),(\alpha.\alpha 3n)]$ /7/. The reactions $[^{121}Sb(\alpha,n)+^{123}Sb(\alpha,3n)]$ and $[^{121}Sb(\alpha,2n)+^{123}Sb(\alpha,4n)]$ are separated with the help of theoretical cross sections. Whereas for the reaction $[^{121}Sb(\alpha,\alpha n)+^{123}Sb(\alpha,\alpha 3n)]$, we have measured only meta state cross section. Hence it is not possible to separate out this reaction using theoretical cross section .To the best of our knowledge , excitation function for this reactions are reported for the first time.

The salient features of the reaction studied are presented below :

IV.2.1 Excitation function of the $[^{121}Sb(\alpha,n)+^{123}Sb(\alpha,3n)]$ ^{124}I reactions :

Consequent on the use of natural antimony target, the isotopic contributions arise in the production of a given final nucleus, such as for example ^{124}I formed via $^{121}Sb(\alpha,n)$ and $^{123}Sb(\alpha,3n)$ reactions jointly. Therefore the experimental cross section in this case gives the weighted average cross section for the two reactions $^{121}Sb(\alpha,n)$ and $^{123}Sb(\alpha,3n)$. Below the threshold energy of $^{123}Sb(\alpha,3n)$ (i.e. 24.4 MeV), the measured cross section is due to $^{121}Sb(\alpha,n)$ reaction only. The relative contribution of the two reactions above 24.4 MeV was separated at each energy point using theoretical excitation function calculations based on preequilibrium model, which predicts the shape and absolute value of the experimentally measured excitation functions.

These reactions were previously studied by Calboreanu et al (1982) , Ismail et al (1989), Singh et al (1991) and Bhardwaj et al (1994) using natural antimony

and stacked foil activation technique. Calboreanu et al /8/ measured $^{121}Sb(\alpha,n)$ reaction up to 27 MeV with an error of 20%.Ismail et al /9/ reported this reaction up to 58 MeV with an error of 8% using Ge(Li) detector, Singh et al /10/ studied this reaction in the energy range 30-60 MeV using Ge(Li) detector with an error of 10% and Bhardwaj et al /11/ also studied this reaction upto 55 MeV using HPGe detector with an error of 10% .There are large variance among all these results. Hence in the present work, the measurements were carried out using a high resolution 120 cc HPGe detector (~2 keV FWHM for 1332 keV photons of ^{60}Co) with an error of less than 7% in the cross section measurements.

The product nucleus ^{124}I was identified by its prominent characteristic 603 and 723 keV gamma rays, having half life 4.15 d and spin 2^-. A typical gamma ray spectrum and partial decay scheme are shown in figure IV.13 and IV.14(a) respectively. The weighted average cross section calculated using the following expression with 603 keV gamma ray as shown in figure IV.8.

$$<\sigma>=\bar{A}i\left[\frac{P_1\sigma_1}{A_1}+\frac{P_2\sigma_2}{A_2}\right]$$

Beyond the threshold energy of $^{123}Sb(\alpha,3n)$, namely 24.4 MeV , the contribution due to $^{121}Sb(\alpha,n)$ reaction is separated out using the theoretical ratio of the cross sections for (α,n) and $(\alpha,3n)$ reactions on ^{121}Sb and ^{123}Sb respectively in the eqn.(11) and (12) of chapter III 3.5. It can be seen from figure that our results agreeing well with previous results in higher energy region where as in lower energy region difference is appreciable. A general agreement is noticed within experimental errors. One can see clearly from the shape of excitation function that below 24.4 MeV, the $^{121}Sb(\alpha,n)$ reaction is dominant whereas beyond 24.4 MeV, the $^{123}Sb(\alpha,3n)$ reaction predominates.

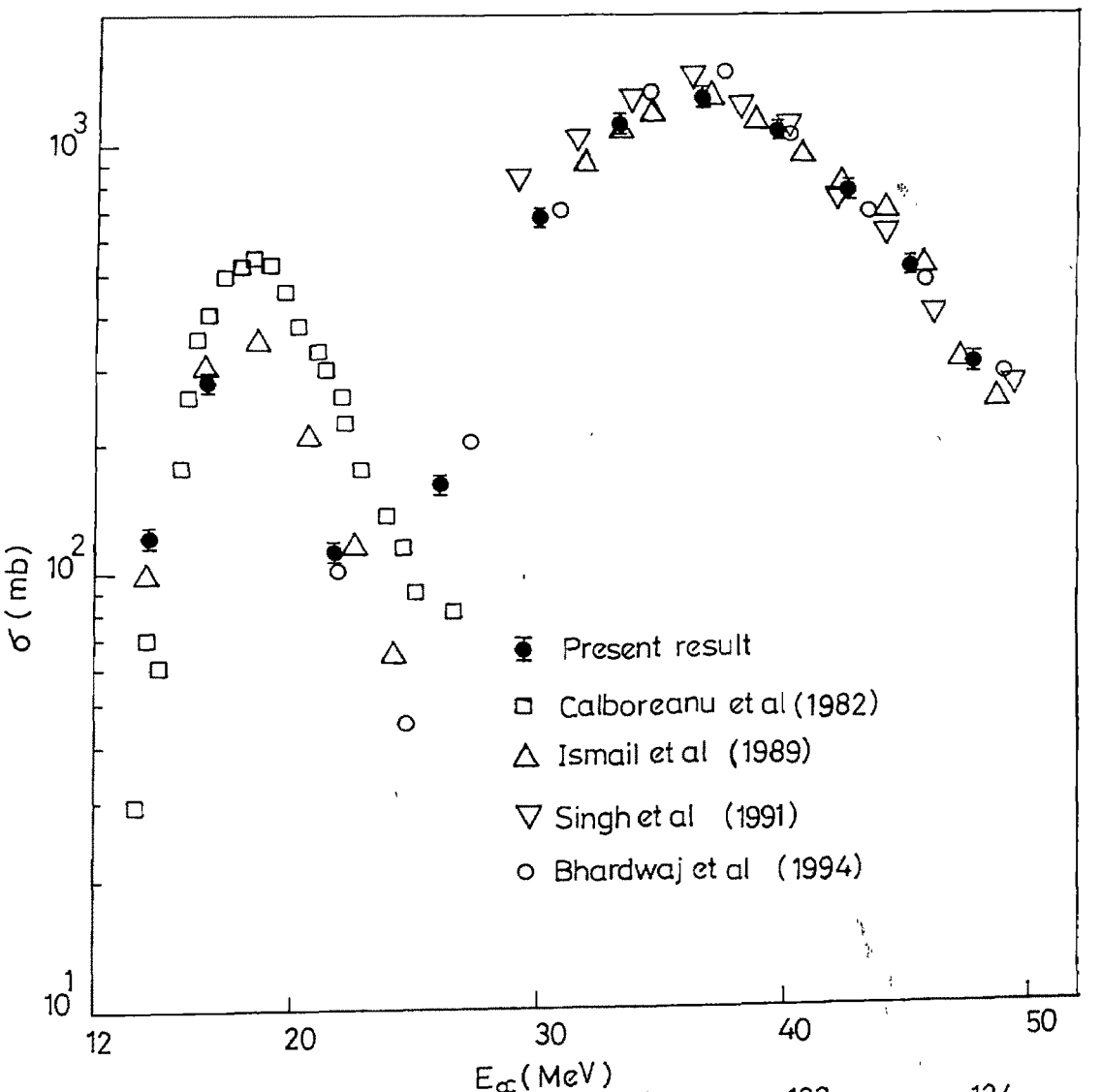

Fig.IV.8 EXCITATION FUNCTION OF [^{121}Sb(α,n) + ^{123}Sb(α,3n)]^{124}I REACTION

IV.2.2 Excitation function of the [^{121}Sb(α,2n)+^{123}Sb(α,4n)] ^{123}I reactions :

As similar to the previous case, the residual nucleus ^{123}I is formed through both ^{121}Sb(α,2n) and ^{123}Sb(α,4n) reactions with threshold energies 15.83 MeV and 32.11 MeV respectively. This product nucleus was identified by its characteristic 159 and 529 keV gamma rays. The residual nucleus ^{123}I having half life 13.02 h and spin $5/2^{+}$. A typical gamma ray spectrum and partial decay scheme are shown in the figure IV.13 and IV.14(b) respectively. The weighted average cross sections were calculated with 159 keV gamma ray using the expression given in the previous case(chapter III.3.5). We have separated the contribution of ^{121}Sb(α,2n) reaction from that of ^{123}Sb(α,4n) reaction beyond 32.11 MeV, using the theoretical cross sections value of ^{121}Sb(α,2n) and ^{123}Sb(α,4n) reactions.

previously , Calboreanu et al /8/ measured only ^{121}Sb(α,2n) reaction whereas another three authors measured both of these reaction in the different energy region. It can be seen from figure IV.9 that there is a fair agreement between present measurement and those of Ismail et al /9/, there are some disagreement between the present results and those of singh et al /10/ and Bhardwaj et al /11/ at higher energy region. The uncertainty in the measurement is less than 7%, which gives the better shape of excitation function. However the above mentioned error does not include the uncertainties of the nuclear data used in the analysis.

IV.2.3 Excitation function of the ^{121}Sb(α,4n)^{121}I reaction :

This reaction previously measured by Ismail et al (1989), Singh et al(1991) and Bhardwaj et al (1994) using natural antimony employing Ge(Li) detector and

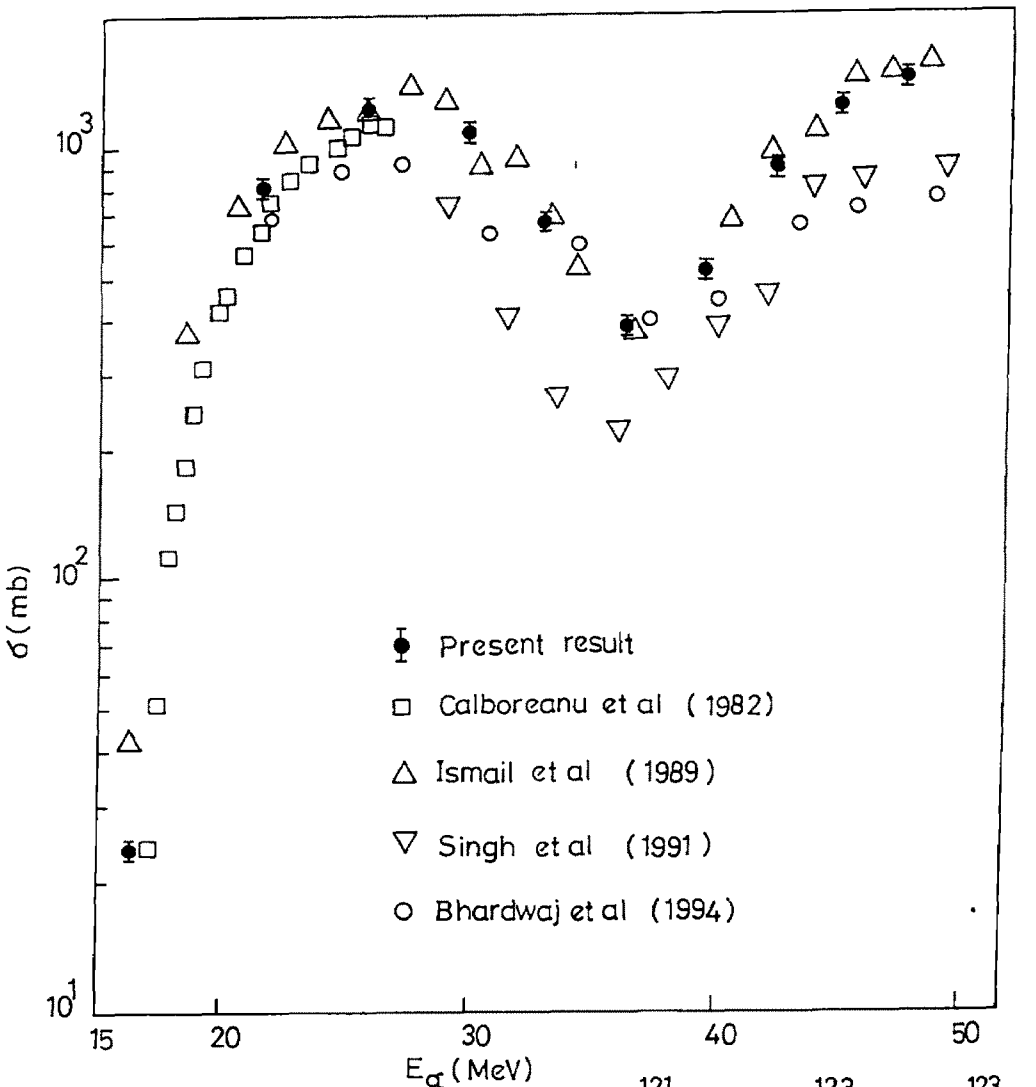

Fig IV.9 EXCITATION FUNCTION OF [^{121}Sb(α,2n) + ^{123}Sb(α,4n)]^{123}I REACTION

HPGe detector . There are discrepancies among the previous results, the reported value of Ismail et al /9/ differs by more than 30% in the higher energy region to those of Singh et al /10/ and Bhardwaj et al /11/ .Hence to improve the quality of data for this reaction , it is reinvestigated using a 120 cc HPGe detector having a excellent resolution (~ 2.0 keV FWHM for 1332 keV photons of ^{60}Co). The product nucleus was identified by its characteristic 212 and 319 keV gamma rays, having half life 2.12 h and spin $5/2^{+}$. A typical gamma ray spectrum and partial decay scheme are shown in figure IV.13 and IV.14(c) respectively.

It can be seen from figure IV.10 that in view of the large threshold energy (34.2 MeV) for this reaction, the compound nucleus mechanism dominates. It is interesting to debate in a multineutron emission reaction like the present one, how many of the four neutrons could still be evaporated at these excitation energies. These questions are discussed in the next chapter which exclusively deals with a comparison of the experimental results and theoretical model predictions.

IV.2.4 Excitation function of the ^{121}Sb(α,p3n)^{121}Te reaction :

Of all nuclear particles neutrons are the easiest to come out of an excited nucleus because they do not feel the Coulomb barrier . Protons and other charged particles have to surmount the Coulomb barrier or penetrate through it, before they can be emitted. Consequently their probability of emission is small compared to that of neutrons. Naively, as the thumb rule, one can say that the cross sections of the reaction involving neutrons, protons and α-particles generally decreases by an order of magnitude down the ladder. For example, the cross section of ^{121}Sb(α,p3n) reaction is 10 times smaller than that of ^{121}(α,4n) reaction at comparative energies.

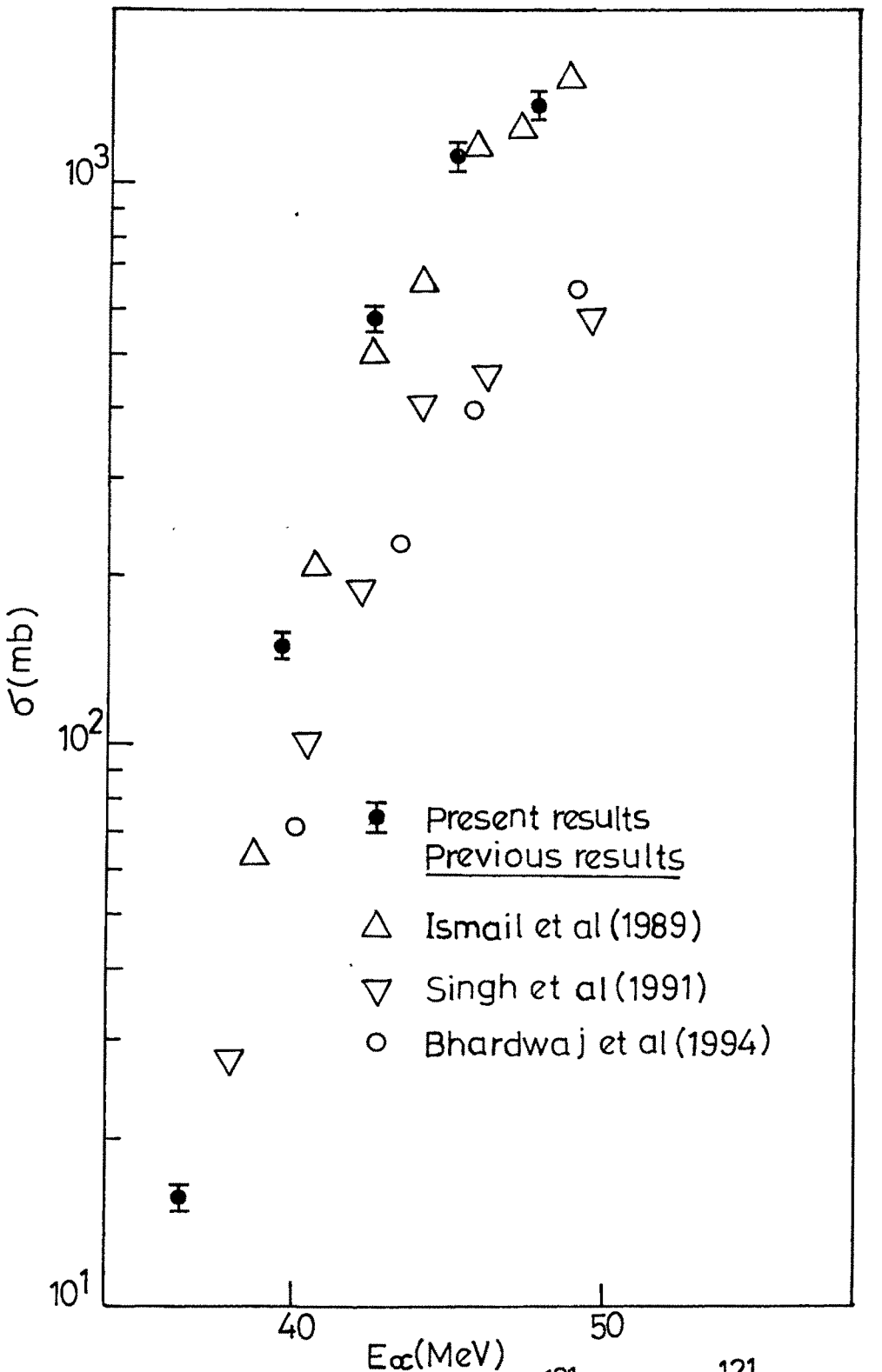

Fig.IV.10 EXCITATION FUNCTION OF $^{121}Sb(\alpha,4n)^{121}I$ REACTION

A case to point out is the pair of reactions : $^{121}Sb(\alpha,4n)^{121}I$ and $^{121}Sb(\alpha,p3n)^{121}Te$. Both the products being neutron deficient isotopes, naturally the isobar with higher Z decays to lower Z by β^+ emission and/or electron capture. Thus, since both these reactions are energetically possible (their threshold differ by a couple of MeV) in the activation measurements, the cross section determined for the lower Z isobar always include the contribution from higher Z isobar. The interfering contribution to the (α,p3n) cross section from that of (α,4n) reaction is really a major problem. In view of the fact that the latter cross section is generally ten times larger than the former.

The product nucleus ^{121}Te which has two isomers of half lives 16.78 d with spin $1/2^+$ (^{121g}Te) and 154 d spin $11/2^-$ (^{121m}Te) respectively. The meta stable state decays to 90% to ground state. In the present case the time of bombardment of the stack was very short in comparison of the half life of meta stable state, so this state could not be excited. The residual nucleus ^{121g}Te was identified by its characteristic 573 and 508 keV gamma rays. A typical gamma ray spectrum and partial decay scheme are shown in figure IV.13 and IV.14(d) respectively. The cross sections were calculated using 573 keV gamma ray. Figure IV.11 shows the present and previous experimental results. It can be seen from the figure that our results agreeing well with Ismail et al /9/.

IV.2.5 Excitation function of the [$^{121}Sb(\alpha,\alpha n)+^{123}Sb(\alpha,\alpha 3n)$] ^{120}Sb reactions :

In the study of α-particle induced reactions in which an α-particle is in the outgoing channel instead of a nucleon have much less probability not only because of the enhanced Coulomb barrier but also due to other factors, such as for instance , the question whether the α-particles pre-exist in the nucleus or formed at the time of

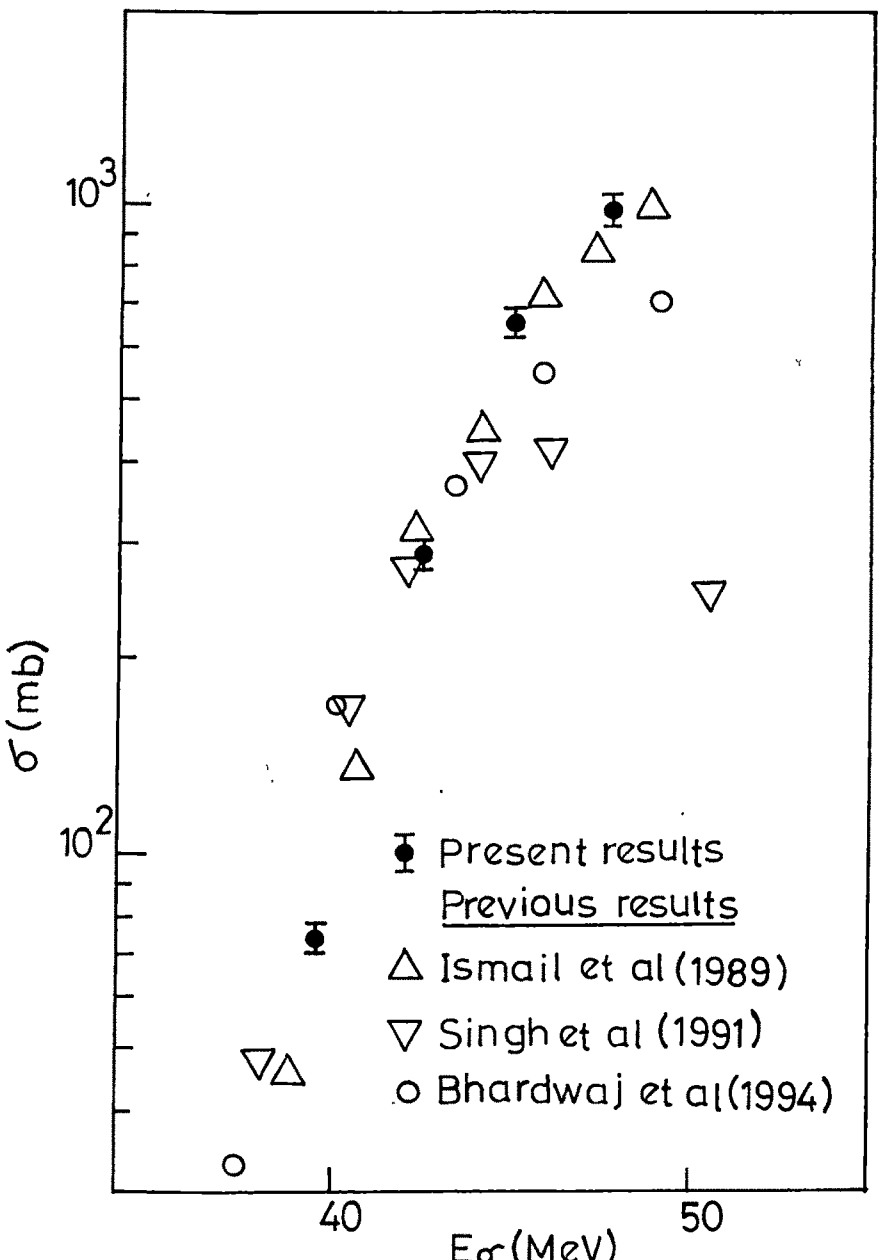

Fig.IV.11 EXCITATION FUNCTION OF $^{121}Sb(\alpha,p3n)^{121}Te$ REACTION

their emission. Though the cross sections are small, it is interesting to study ($\alpha,\alpha xn$) type of reactions from the emission mechanism point of view.

To the best of our knowledge, the excitation function for $^{121}Sb(\alpha,\alpha n)$ + $^{123}Sb(\alpha,\alpha 3n)$ reactions are reported for the first time. The two ^{120}Sb isomers are produced in the $^{121}Sb(\alpha,\alpha n)$ + $^{123}Sb(\alpha,\alpha 3n)$ reactions with spins 8^- and 1^+ having half lives of 5.76 d and 15.8 m respectively. They are genetically independent isomeric states. We have measured the cross section for the isomeric state having half life 5.76 d. The product nucleus was identified by its characteristic 1023 and 1172 keV gamma rays. A typical gamma ray spectrum and partial decay scheme are shown in figure IV.13 and IV.14(e) respectively. The cross sections were calculated using 1172 keV gamma ray as shown in figure IV.12.

A complete summary of the results obtained in the present experimental study is given in table IV.2.

IV. 3 Alpha Particle Induced Reactions in the Target Element Indium :

Indium is a typical element situated in the middle of the periodic table having two odd mass stable isotopes of abundances 4.3% (^{113}In) and 97.6%(^{115}In). In principle, it is possible that same residual nucleus may be formed through different isotopes during alpha particle bombardment. However, more often than not, it turns out that at a given energy only one of the two reaction channels, is predominant and the other is a small contribution. One of the two vanishes, if the energy happens to be less than the threshold energy for that reaction. On this basis, the experimentally measured weighted average cross section can be easily interpreted using the formula

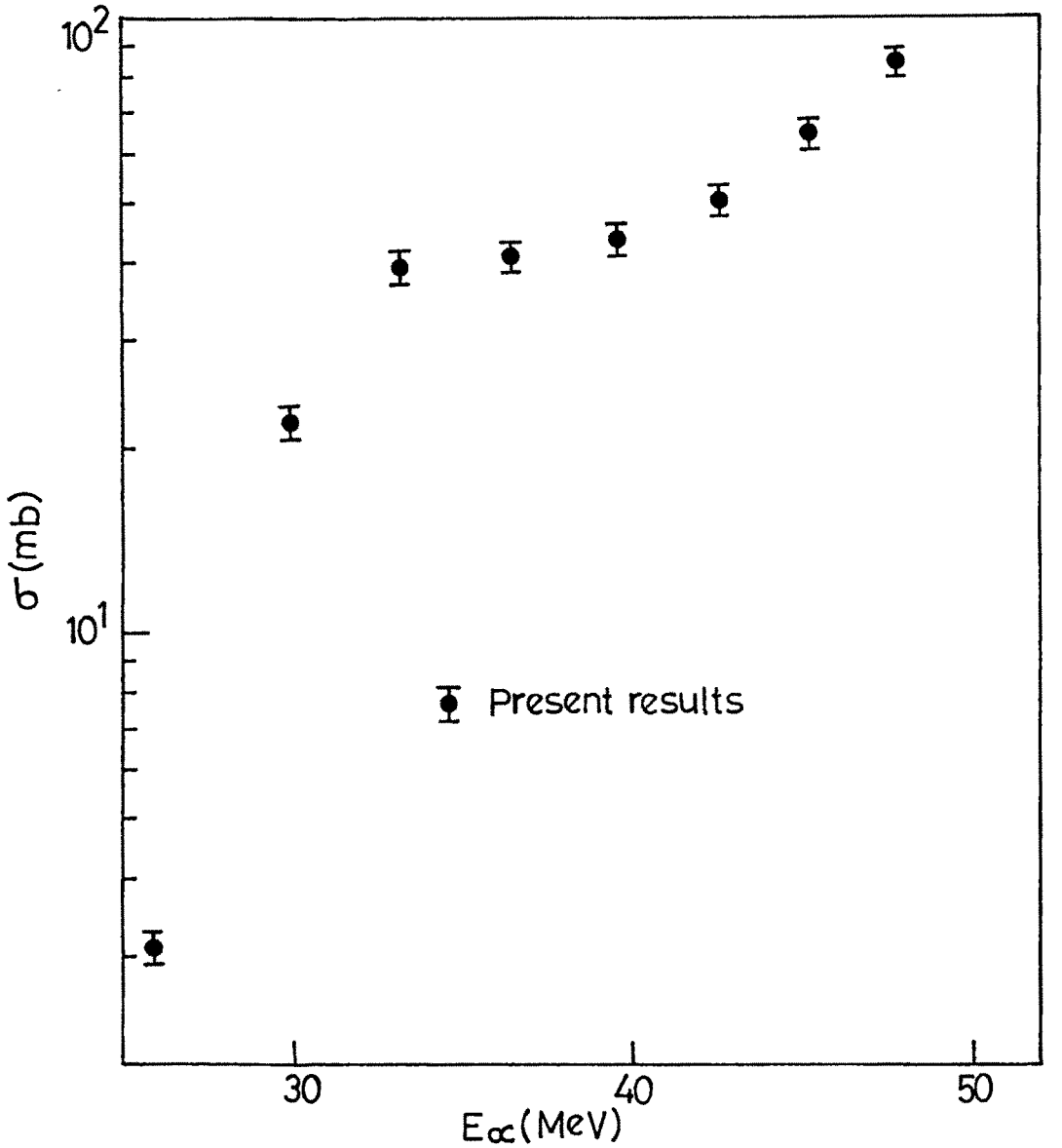

Fig. IV.12 EXCITATION FUNCTION OF $[^{121}Sb(\alpha,\alpha n)+^{123}Sb(\alpha,\alpha 3n)]^{120}Sb$ REACTION

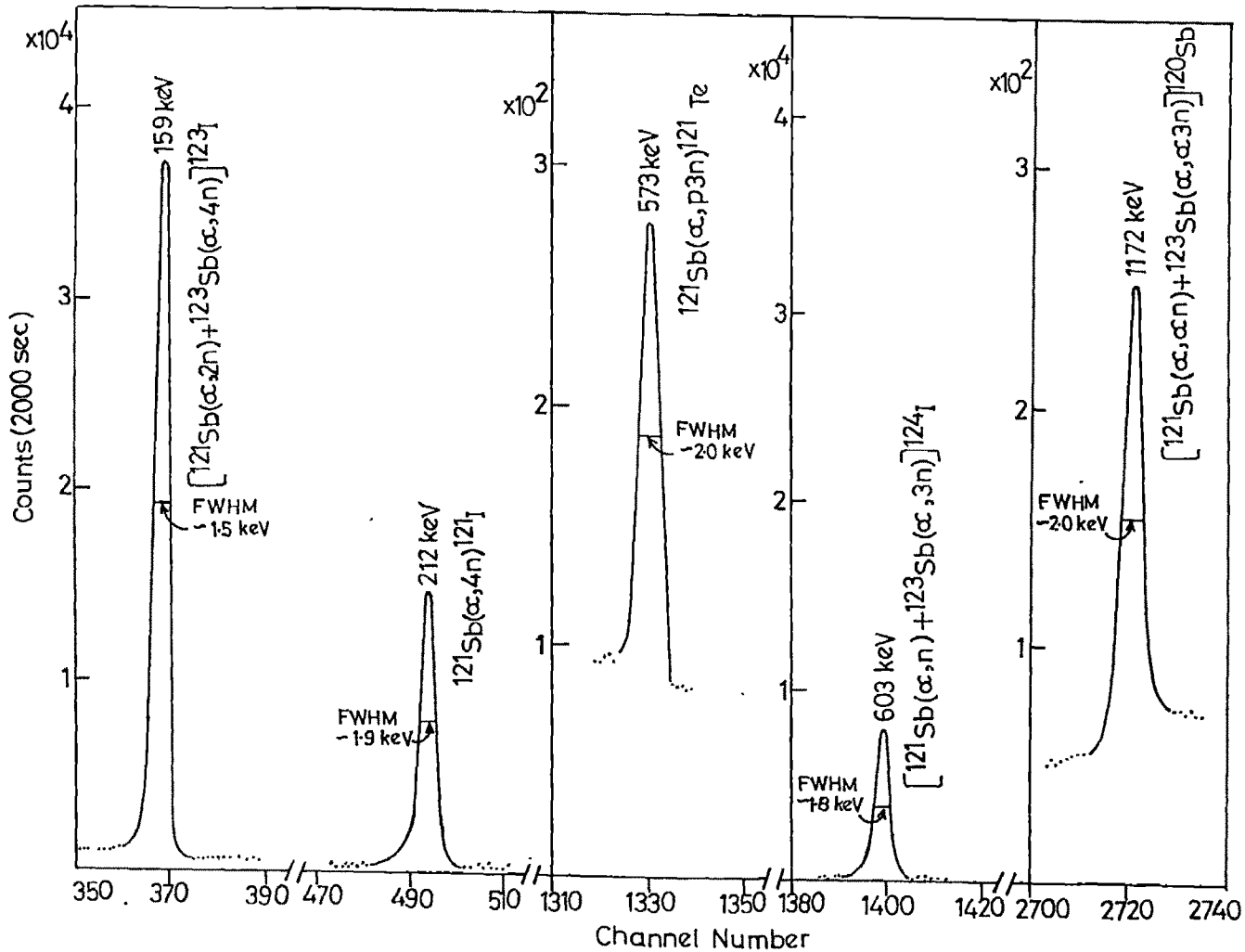

Fig.IV.13 A TYPICAL GAMMA RAY SPECTRUM OF ACTIVATED SAMPLE OF ANTIMONY

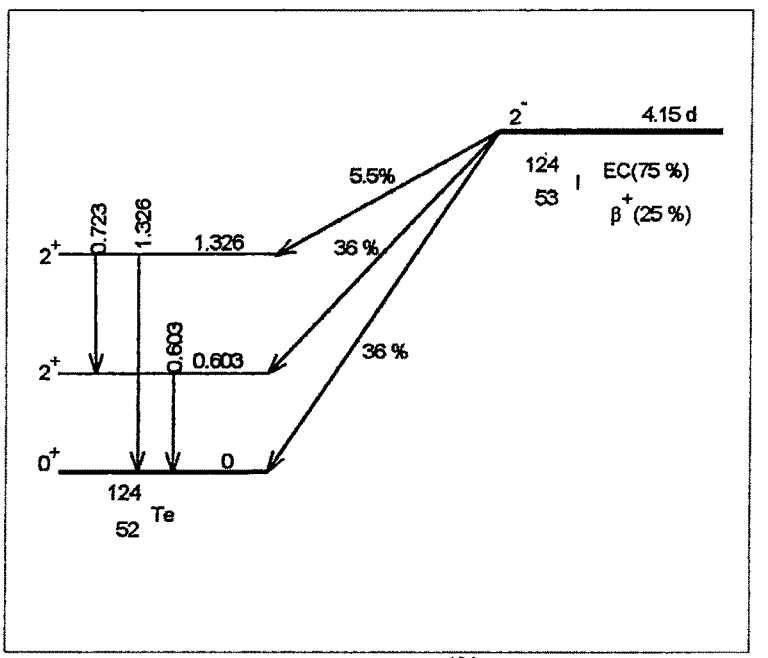

Fig.IV.14(a) Partial decay scheme of ^{124}I

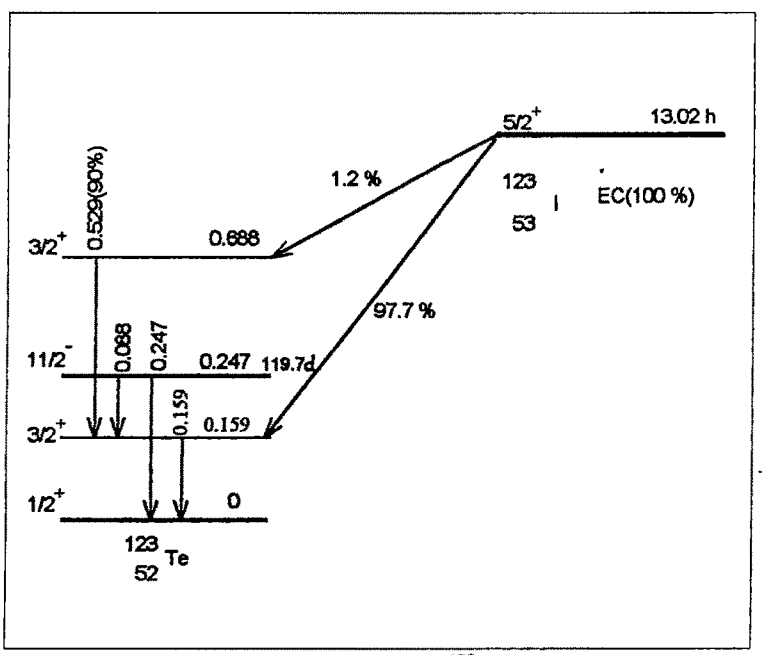

Fig.IV.14(b) Partial decay scheme of ^{123}I

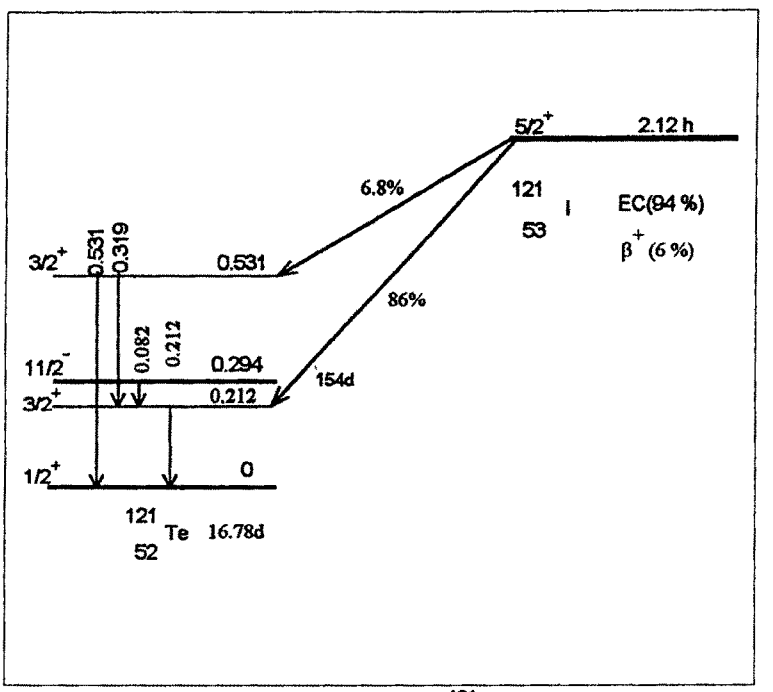

Fig.IV.14(c) Partial decay scheme of ^{121} I

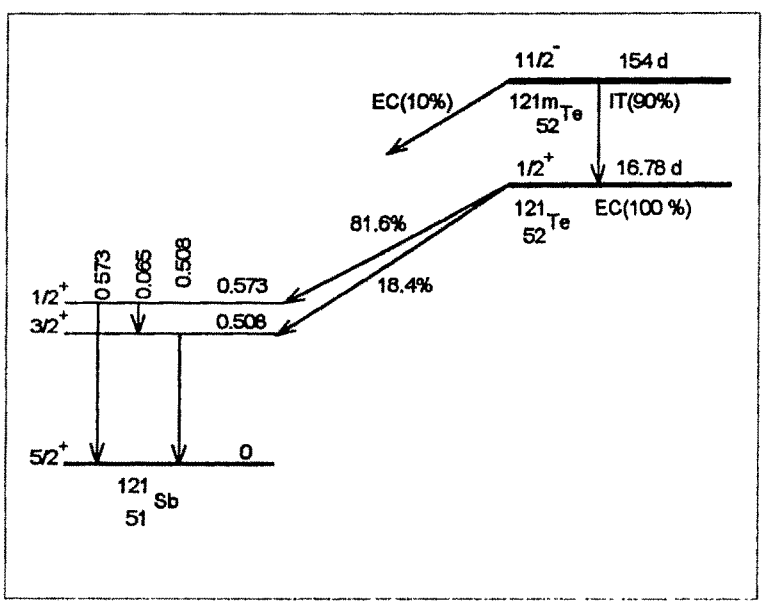

Fig.IV.14(d) Partial decay scheme of ^{121} Te

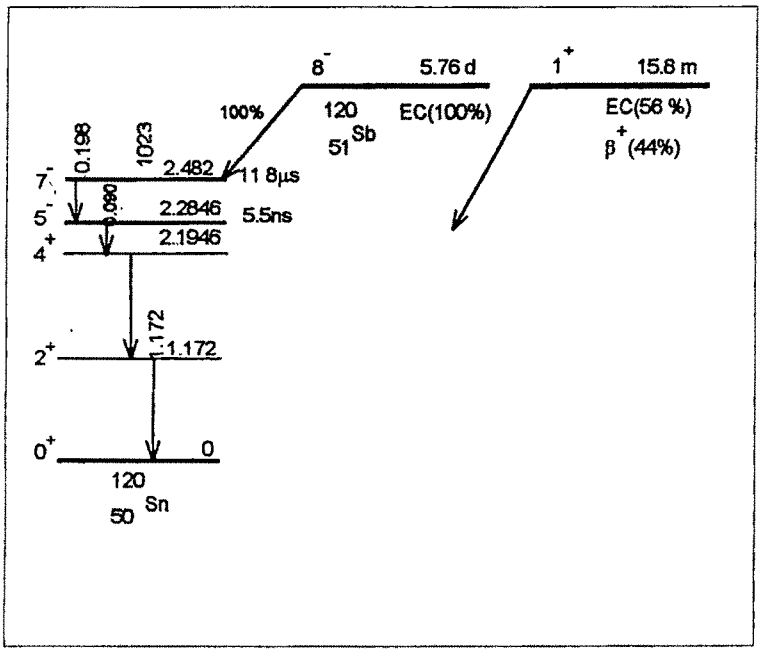

Fig.IV.14(e) Partial decay scheme of ^{120}Sb

Table IV.2 Cross sections of the α-induced reaction on ^{121,123}Sb measured in the present work.

Reaction	**^{121}Sb(α,n)**	**^{121}Sb(α,2n)**	**^{121}Sb(α,4n)**	**^{121}Sb(α,p3n)**	**^{123}Sb(α,3n)**	**^{123}Sb(α,4n)**	**^{121}Sb(α,αn) + ^{121}Sb(α,α3n)**
Product nucleus	**^{124}I**	**^{123}I**	**^{121}I**	**^{121}Te**	**^{124}I**	**^{123}I**	**^{120}Sb**
Threshold energy (MeV)	**08.13**	**15.83**	**34.42**	**31.17**	**24.40**	**32.11**	**09.53 25.82**
$E_α$(MeV)	**σ(mb)**	**σ(mb)**	**σ(mb)**	**σ(mb)**	**σ(mb)**	**σ(mb)**	**σ(mb)**
14.2	122.0±6.22						
16.5	280.9±14.3	23.4±1.3					
21.7	112.9±5.76	809.6±46.5					
25.9	41.0±2.1	1207.0±69.3			120.2±6.1		3.1±0.2
29.9	21.6±1.1	1069.0±61.4			658.2±33.5		22.1±1.4
33.1	15.5±0.8	637.2±36.6			1096.3±55.8	32.6±1.9	39.0±2.4
36.4	12.8±0.6	238.6±13.7	15.6±0.9		1283.5±65.3	146.8±8.4	41.3±2.5
39.5	10.8±0.5	117.6±6.7	148.2±8.5	73.9±4.2	1066.5±54.3	396.6±22.8	42.7±2.6
42.5	9.3±0.5	93.4±5.4	576.7±33.1	288.3±16.5	771.3±39.2	786.4±45.1	49.5±3.0
45.1	8.3±0.4	79.9±4.6	1102.0±63.2	657.9±37.8	513.0±26.1	1131.9±65.0	63.6±3.9
47.7	7.2±0.4	68.3±3.9	1350.0±77.5	981.2±56.3	304.0±15.5	1338.6±76.8	82.7±5.1

$$<\sigma>= \bar{A}i\left[\frac{P_1\sigma_1}{A_1}+\frac{P_2\sigma_2}{A_2}\right]$$

where $\bar{A}_i$ is the average mass number of the indium, P_1 A_1 and P_2 A_2 are the percentage abundance and mass number of the two isotopes of indium in respective order; σ_1 and σ_2 are the individual cross sections of the reactions from ^{113}In and ^{115}In isotopes, respectively. The two contributions can be separated quite accurately using the theoretical excitation function in the eqns. 11 & 12 , chapter III.3.5.

In the present work, excitation functions for the reactions ^{115}In[(α,n),(α,2n),(α,3n),(α,2p)] and ^{113}In(α,n) have been studied upto 50 MeV using stacked foil activation technique/12/. Previously Mukherjee et al /15/ and Hansen and Stelts /13/ had confined only to the (α,xn) reactions upto 50 MeV and 18 MeV using Ge(Li) and poor resolution scintillation detector respectively. While Bhardwaj et al /14/ measured all above reactions using a Ge(Li) detector upto 50 MeV. In view of large discrepancies in these measurements, a reinvestigation of the above reaction was undertaken to improve the quality of experimental data.

The salient features of these reactions studied are discussed below:

IV.3.1 Excitation function of the [^{113}In(α,n)+^{115}In(α,3n)]^{116m}Sb reaction :

In the present work, the two reactions ^{113}In(α,n)+^{115}In(α,3n) lead to the same residual nucleus ^{116}Sb. Since the threshold of ^{113}In(α,n) and ^{115}In(α,3n) reactions are different but even then there is some region in which both the reactions go on simultaneously . The cross sections in the overlapping energy region can be separated out accurately using theoretical cross sections in the formulation given in

the chapter III.3.5, eqns.(11) and (12). However the present measurement is only for meta stable state, so that above mentioned formula can not be used.

The product nucleus ^{116}Sb has a meta stable state and ground state of half lives 60.42 m (spin 8$^-$) and 15.5 m (spin 3$^+$) respectively. In the present work we have studied only meta stable state activity, which decays independently through electron capture (81%) and β^+ emission(19%).The product nucleus ^{116m}Sb was identified by its characteristic 543,973 and 1294 keV gamma rays .A typical gamma ray spectrum and partial decay scheme are shown in figure IV.19 and IV.20(a) respectively. In ground state (^{116g} Sb), 72% decay is through electron capture mode while 28% decay is through β^+ emission. As the activity produced in the target foils was very high, so the stack of target foils was cooled down till the activity reached permissible dose rate and this cooling took a long time. So due to long gap between start of counting of the gamma rays and stop of bombarding of target stack, there may not be any contribution of short lived ground state. Hence, the activity due to metastable state only could be observed. The weighted average cross sections for both reactions calculated using 973 keV gamma ray as shown in figure IV.15.

Previously this reaction was measured by Bhardwaj et al /14/ and Mukherjee et al /15/ .It is quite evident from figure that disagreement between the Bhardwaj et al and Mukherjee et al is more than an order of magnitude in high energy region. Whereas the present results are in good agreement with Bhardwaj et al. The error in measurement is less than 7%.

IV.3.2 Excitation function of the ^{115}In(α,n)^{118m}Sb reaction :

This reaction was studied earlier by Hansen and Stelts /13/ in the energy range 12 to 18 MeV using poor resolution detector. Bhardwaj et al /14/ measured

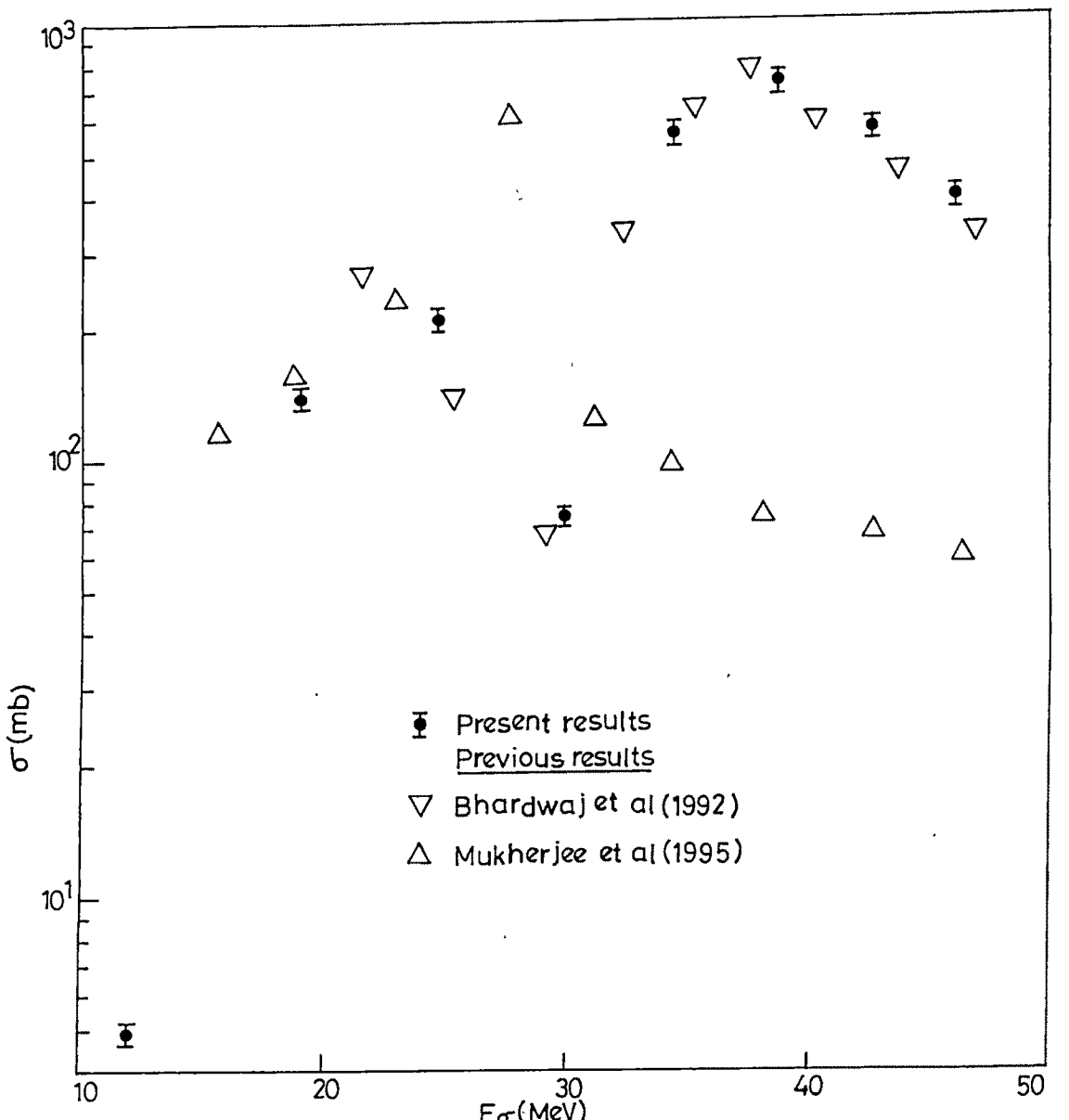

Fig.IV.15 EXCITATION FUNCTION OF $[^{113}In(\alpha,n)+^{115}In(\alpha,3n)]^{116m}Sb$ REACTION

this reaction upto 50 MeV using Ge(Li) detector with an error of less than 12%. Mukherjee et al /15/ also studied this reaction using Ge(Li) detector upto 50 MeV with an error of 9 to 14%.These two measurements show a large deviation in the cross section at high energies.

Hence in the present work we have made systematic reinvestigation of this reaction employing 120 cc HPGe detector having a resolution 2 keV for 1332 keV photons of ^{60}Co. In this reaction the product nucleus ^{118}Sb has a ground state and meta stable state of half lives 3.5 m (spin 1^+) and 5.0 h (spin 8^-) respectively. The meta stable state of ^{118}Sb decays to the level ^{118}Sn through electron capture (99.84%) and β^+ emission (0.16 %). The decay of ground state is also through the electron capture(22.5%) and β^+ emission (75%). The half life of the ground state ^{118g}Sb is very short, therefore the observed activity was due to meta stable state only. A typical gamma ray spectrum and partial decay scheme are shown in figure IV.19 and IV.20(b) respectively.

The cross sections were calculated using 1230 keV gamma rays as shown in figure IV.16. It can be seen from figure that our results agree well with Bhardwaj et al at higher energy region than those of Mukherjee et al. However it is well matched with Mukherjee et al in the compound nucleus region.

IV.3.3 Excitation function of the ^{115}In(α,2n)^{117}Sb reaction :

The residual nucleus ^{117}Sb having half life 2.8 h and spin $5/2^+$, was identified by its characteristic 159, 861 and 1020 keV gamma rays , which decays independently through electron capture (97.5%) and β^+ emission (2.5%).A typical gamma ray spectrum and partial decay scheme are shown in figure IV.19 and IV.20(c) respectively.

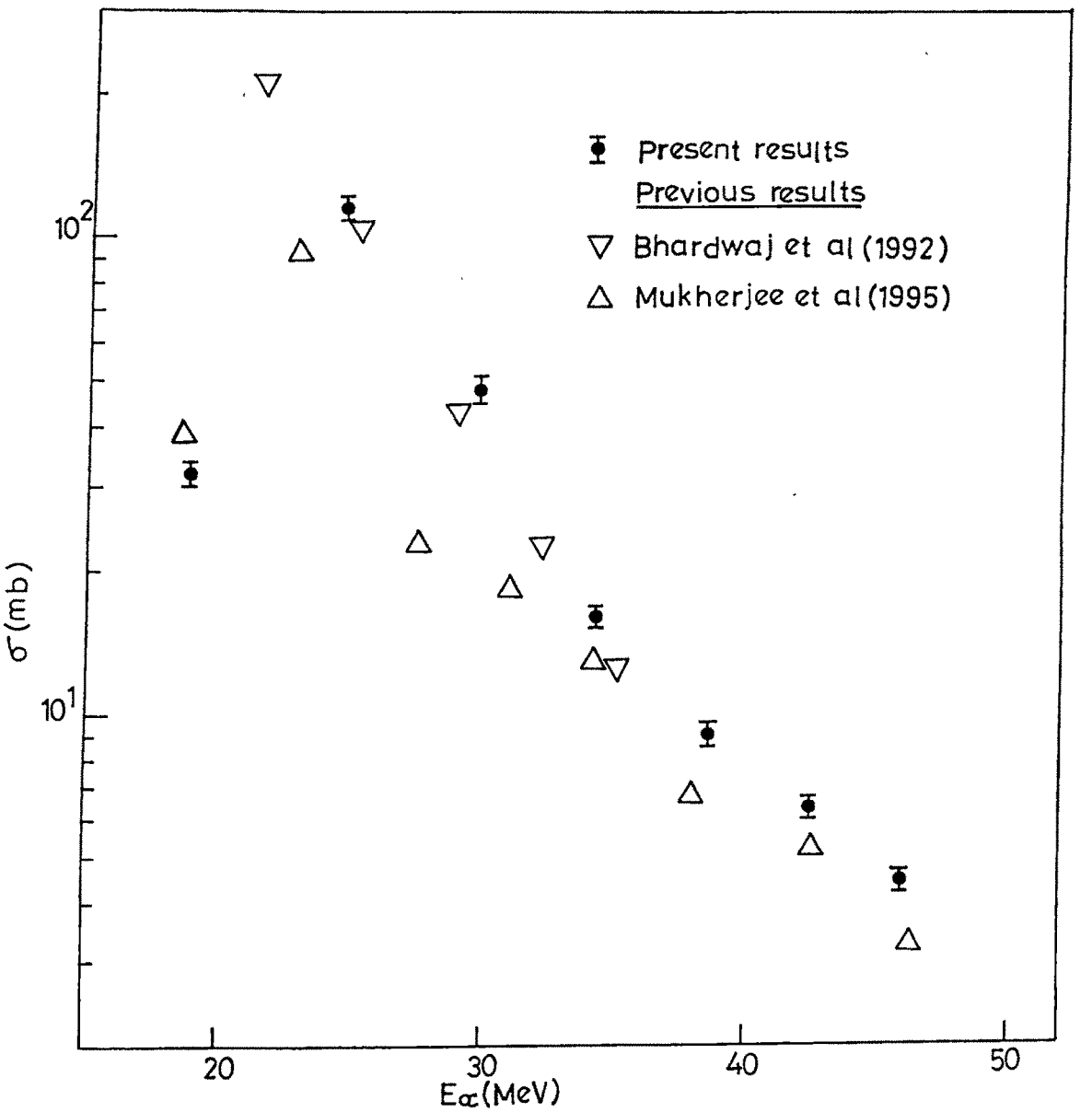

Fig.IV.16 EXCITATION FUNCTION OF $^{115}In(\alpha,n)^{118m}Sb$ REACTION

This reaction was earlier studied by Bhardwaj et al /14/ and Mukherjee et al /15/. The cross sections were calculated using 159 keV gamma rays as shown in the figure IV.17. It can be seen from figure that while there is a fair agreement between present result and those of Bhardwaj et al. There is some disagreement between the present measurement and those of Mukherjee et al by a factor of two at higher energy region.

IV.3.4 Excitation function of the $^{115}In(\alpha,2p)^{117m}In$ reaction :

As discussed earlier, of all nuclear particles neutrons are the easiest to come out of an excited nucleus because they do not feel the Coulomb barrier. Protons and other charged particles have to surmount the Coulomb barrier before they can be emitted. Consequently, their probability of emission is small compared to that of neutrons. Hence generally the cross sections for (α,pxn) reactions are about an order of magnitude smaller than corresponding (α,xn) reactions.

In this reaction the product nucleus ^{117}In has a metastable state and ground state of half lives 1.93 h (spin $1/2^-$) and 42.3 m (spin $9/2^+$) respectively. We have measured only metastable activity. The product nucleus ^{117m}In was identified by its characteristic 315 keV gamma ray. A typical gamma ray spectrum and partial decay scheme are shown in figure IV.19 and IV.20(d) respectively. This reaction previously studied only by Bhardwaj et al /14/. It can be seen from figure IV.18 that the previously reported cross section values beyond 35 MeV are quite over estimated than present one.

A complete summary of the results obtained in the present experimental study is given in the table IV.3.

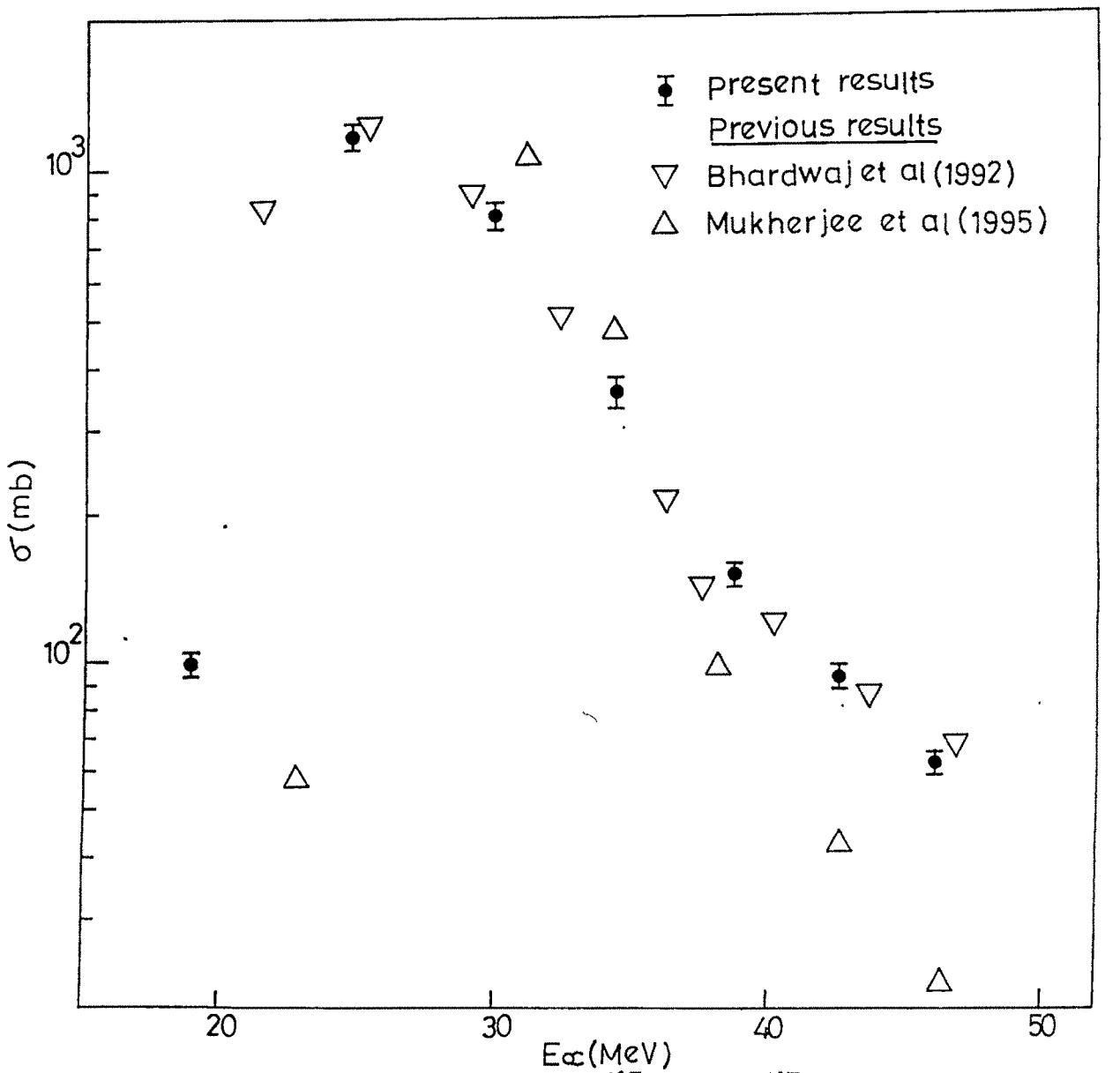

Fig.IV.17 EXCITATION FUNCTION OF $^{115}In(\alpha,2n)^{117}Sb$ REACTION

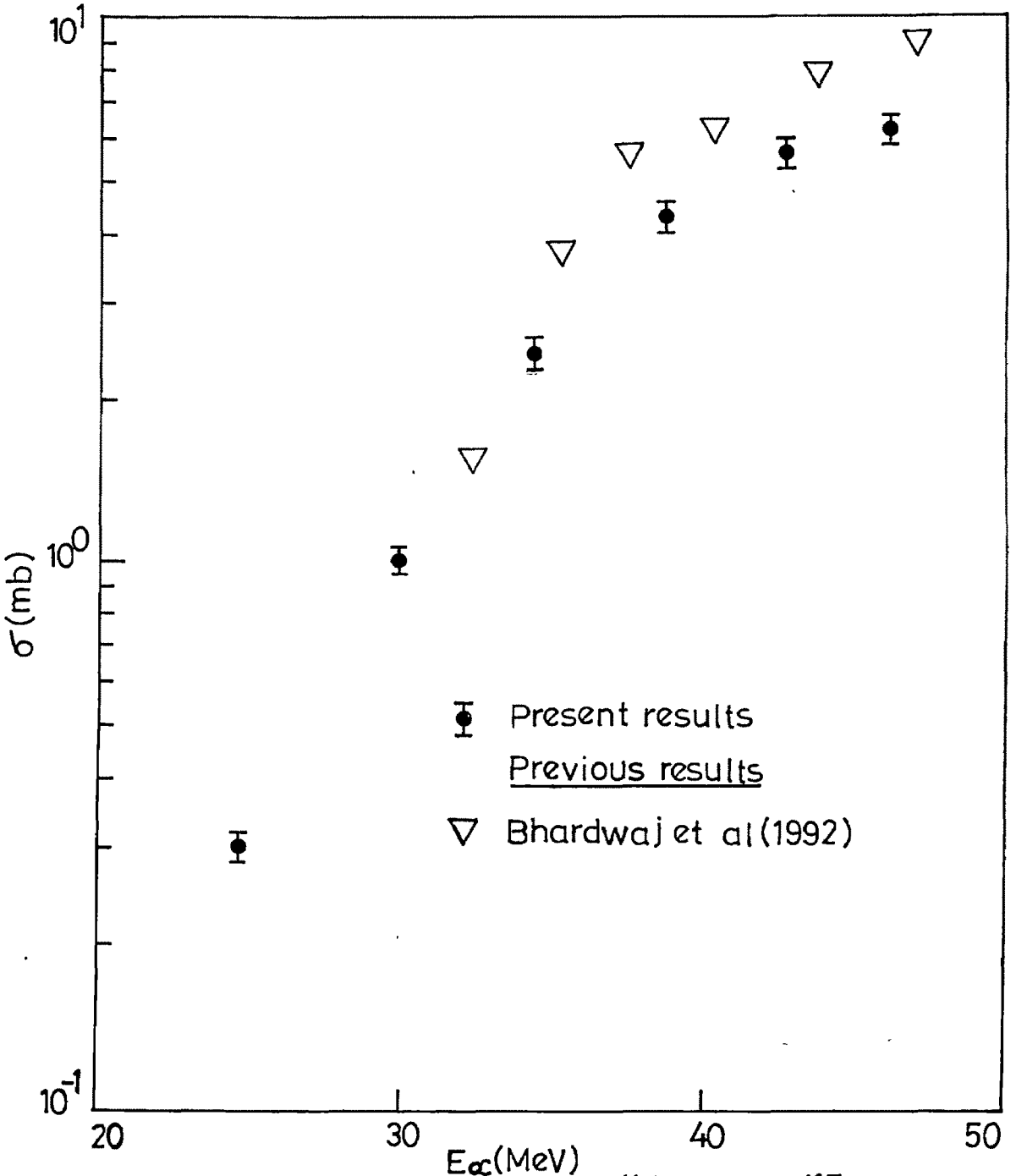

Fig.IV.18 EXCITATION FUNCTION OF $^{115}In(\alpha,2p)^{117m}In$ REACTION

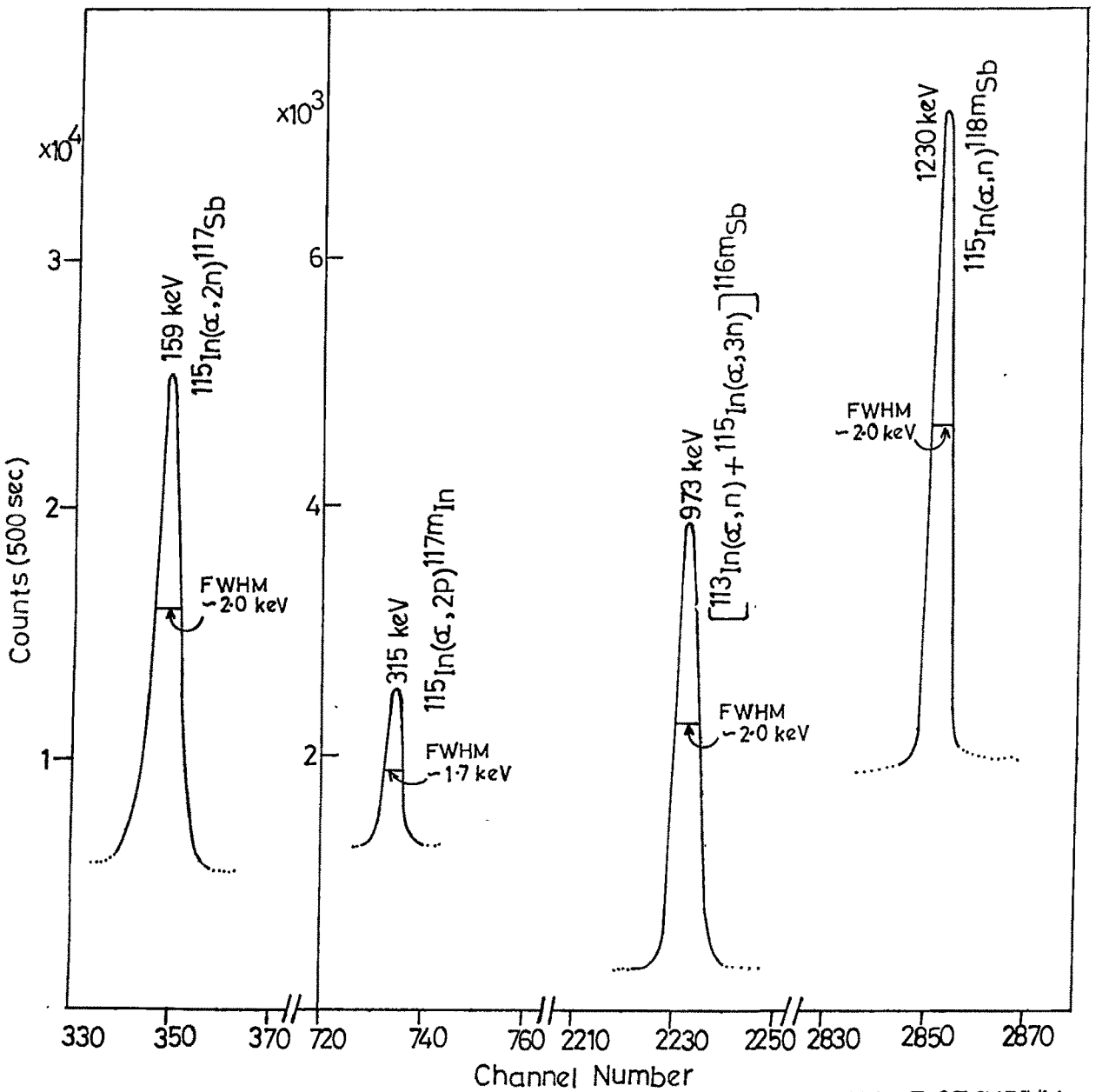

Fig.IV·19 A TYPICAL GAMMA RAY SPECTRUM OF ACTIVATED SAMPLE OF INDIUM

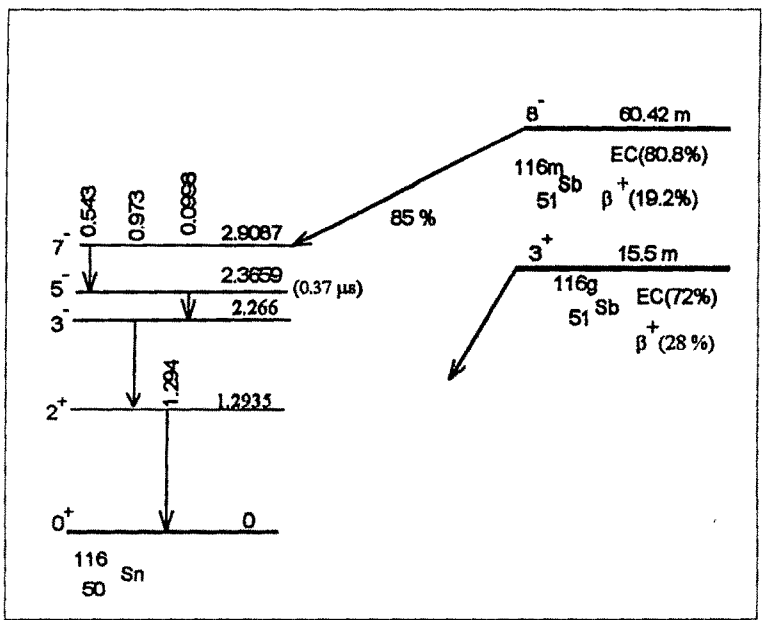

Fig.IV.20(a) Partial decay scheme of ^{116}Sb

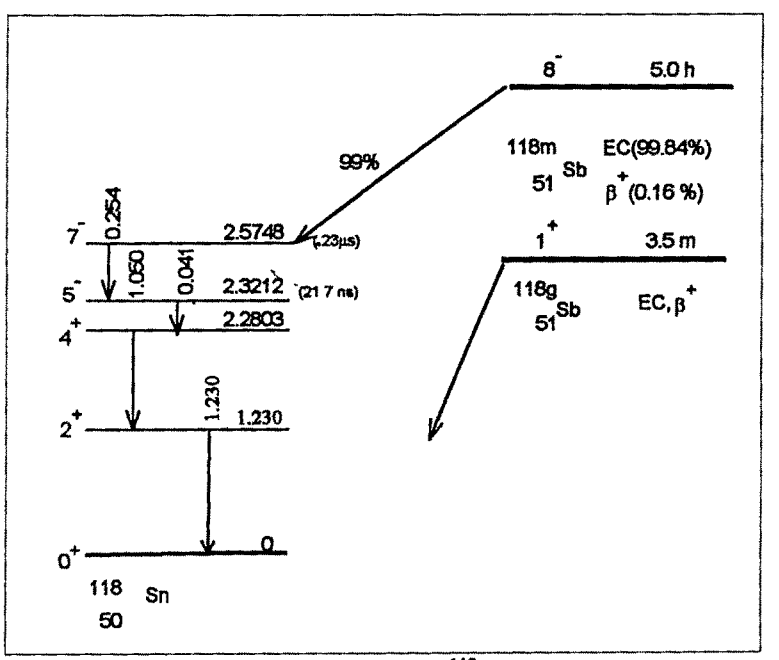

Fig.IV.20(b) Partial decay scheme of ^{118}Sb

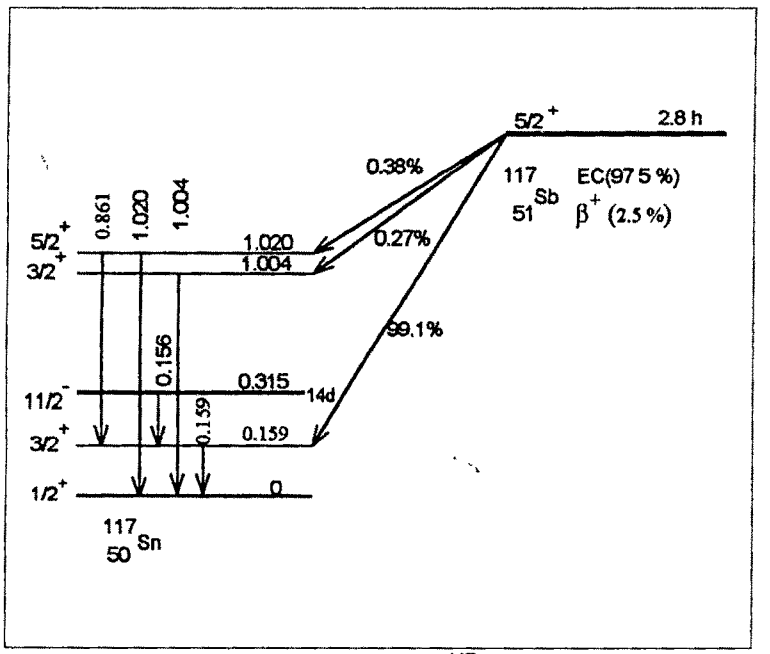

Fig.IV.20(c) Partial decay scheme of ^{117}Sb

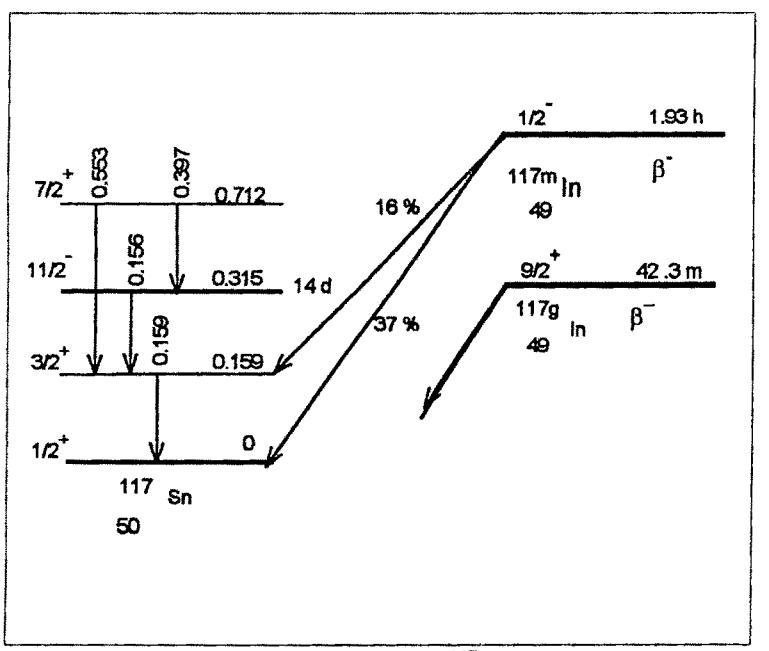

Fig.IV.20(d) Partial decay scheme of ^{117}In

Table IV.3 Cross sections of the α-induced reaction on ^{113,115}In measured in the present work.

Reaction	^{115}In(α,n)	^{115}In(α,2n)	^{115}In(α,3n) +^{113}In(α,n)	^{115}In(α,2p)
Product nucleus	^{118m}Sb	^{117}Sb	^{116m}Sb	^{117}In
Threshold energy (MeV)	07.69	15.10	25.88 08.99	13.51
E_α(MeV)	σ(mb)	σ(mb)	σ(mb)	σ(mb)
12.0			004.9±00.3	
18.9	032.1±1.8	0098.0±04.9	138.0±07.7	
24.6	116.0±7.8	1160.0±77.7	210.0±11.7	0.3±0.01
29.8	048.0±3.2	0799.2±53.5	073.1±03.7	1.0±0.05
34.3	016.2±0.8	0349.1±23.4	549.0±36.8	2.4±0.20
38.6	009.1±0.5	0147.6±08.2	723.4±48.5	4.3±0.30
42.5	006.3±0.3	0091.5±05.1	558.4±37.4	5.6±0.40
46.0	004.4±0.2	0062.3±03.5	390.6±26.2	6.2±0.40

IV. 4 Alpha Particle Induced Reactions in the Target Element Iron :

Natural iron is a multi-isotopic element of abundance 5.8% (^{54}Fe), 91.8% (^{56}Fe), 2.15%(^{57}Fe) and 0.29%(^{58}Fe). In the present work excitation functions for the reactions ^{56}Fe[(α,3n),(α,4n),(α,pn),(α,p2n) and (α,p3n)] have been studied /16/ upto 50 MeV with a view to improve the quality of earlier measurements. All the previous measurements were carried out mostly using poor resolution detector and there were no improved measurements almost during the last decade. Further, in some reactions, the cumulative yield due to the decay of all isobars of the reaction product was measured and no attempt was made to separate them analytically or otherwise. In this scenario, it is felt that there is certainly a need for a systematic reinvestigation of the above reactions using high resolution HPGe detector.

The salient features of the reaction studied are as below:

IV.4.1 Excitation function of the ^{56}Fe(α,3n)^{57}Ni reaction:

This reaction was earlier studied by Tanaka et al /17/ and Ewart et al /18/. Tanaka et al measured this reaction upto 40 MeV using GM counter and scintillation counter with an error of 16% whereas Ewart et al studied this reaction upto 68 MeV employing proportional counter and scintillation detector using enriched ^{56}Fe for $E_\alpha > 43$ MeV and natural iron for $E_\alpha < 43$ MeV respectively. The reported uncertainty in their measurement was less than 20%. Hence in the present work we have reinvestigated this reaction using high resolution (~ 2 keV FWHM for 1332 keV photons of ^{60}Co) HPGe detector with an error of 8%.

The product nucleus ^{57}Ni was identified by its characteristic 1378 and 127 keV gamma rays. The product nuclei having half life 36 h and spin $3/2^-$, which

decays independently through electron capture (60%) and β^+ emission (40%). A typical gamma ray spectrum and partial decay scheme are shown in figure IV.26 and IV.27(a) respectively. The comparison of the present experimental results with those of previous works are shown in figure IV.21. It can be seen that there is an overall agreement between the present results and those of previous results.

IV.4.2 Excitation function of the $^{56}Fe(\alpha, 4n)^{56}Ni$ reaction :

This reaction previously studied only by Ewart et al /18/ in the energy range 50-68 MeV. The uncertainty in the measurement was quoted to be 30%. Since the threshold energy of this reaction is very high, 39.17 MeV and the energy limit in present work is only 50 MeV, we did not compare this reaction with previous measurement. The product nuclei ^{56}Ni having half life 6.1 d and spin 0^+ was identified by its characteristic 158, 480 and 750 keV gamma rays . A typical gamma ray spectrum and partial decay scheme are shown in figure IV.26 and IV.27(b) respectively. The cross section measurement was done using 750 keV gamma ray as shown in figure IV.22.

IV.4.3 Excitation function of the $^{56}Fe(\alpha,pn)^{58}Co$ reaction :

This reaction previously measured by Tanaka et al /17/, Ewart et al /18/ and Vedoya et al /19/. Tanaka et al measured upto 40 MeV employing GM counter and scintillation counter using natural iron. Ewart et al studied upto 68 MeV using proportional counter and scintillation detector with an error of less than 25%. Vedoya et al studied this reaction using Ge detector and natural iron upto 85 MeV with an error varying from 3-16 % . It can be seen in figure IV.23 that there are large mutual disagreement among the previously measured values. Hence in the

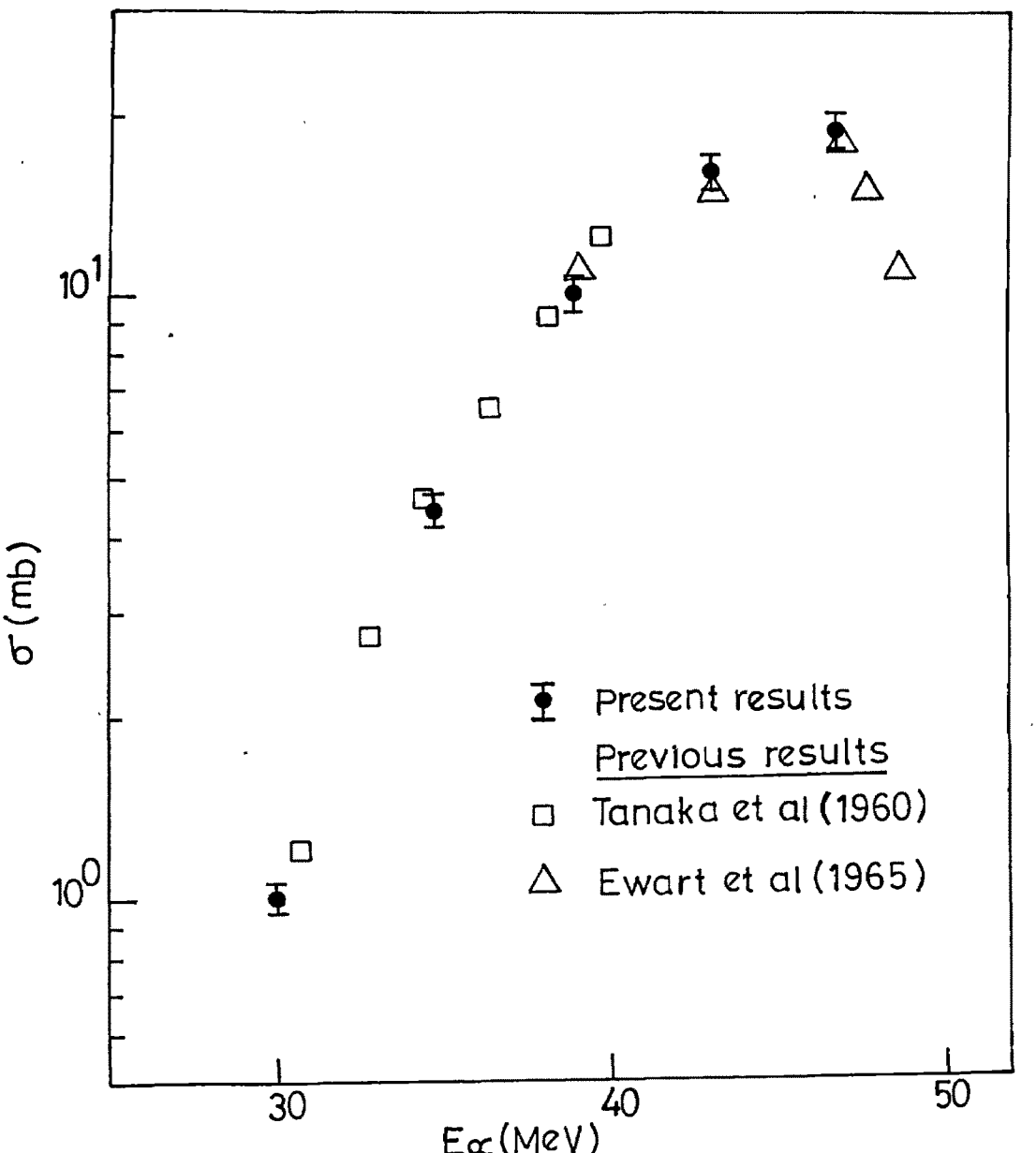

Fig. IV.21 EXCITATION FUNCTION OF $^{56}Fe(\alpha,3n)^{57}Ni$ REACTION

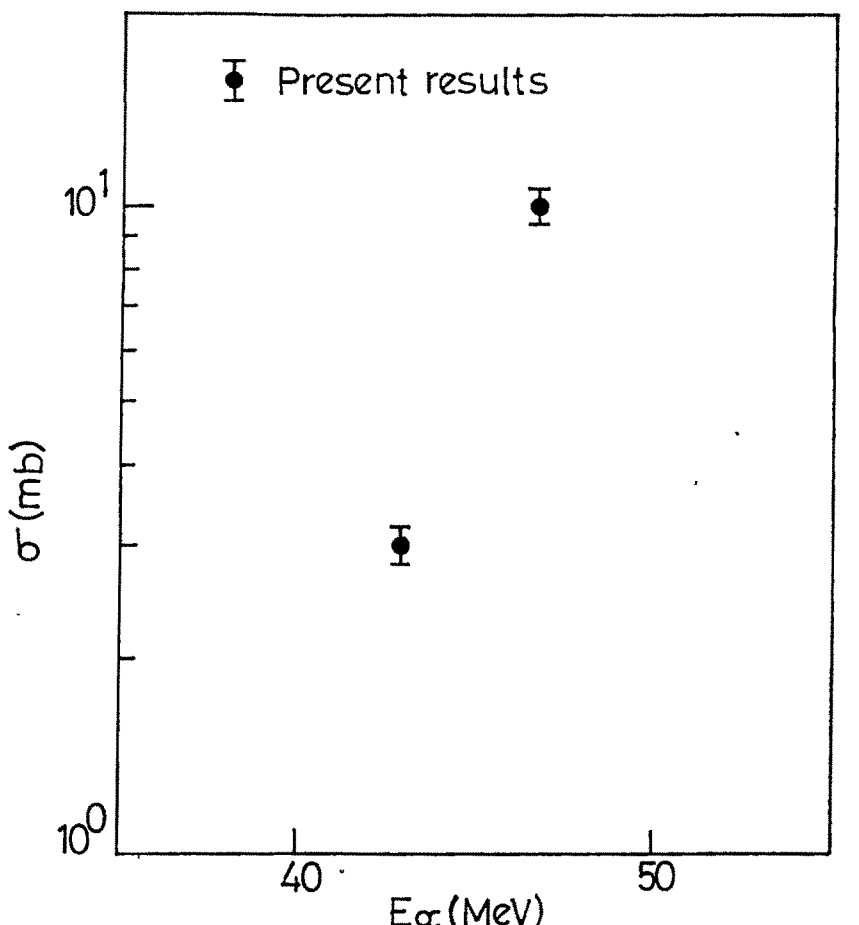

Fig. IV.22 EXCITATION FUNCTION OF $^{56}Fe(\alpha,4n)^{56}Ni$ REACTION

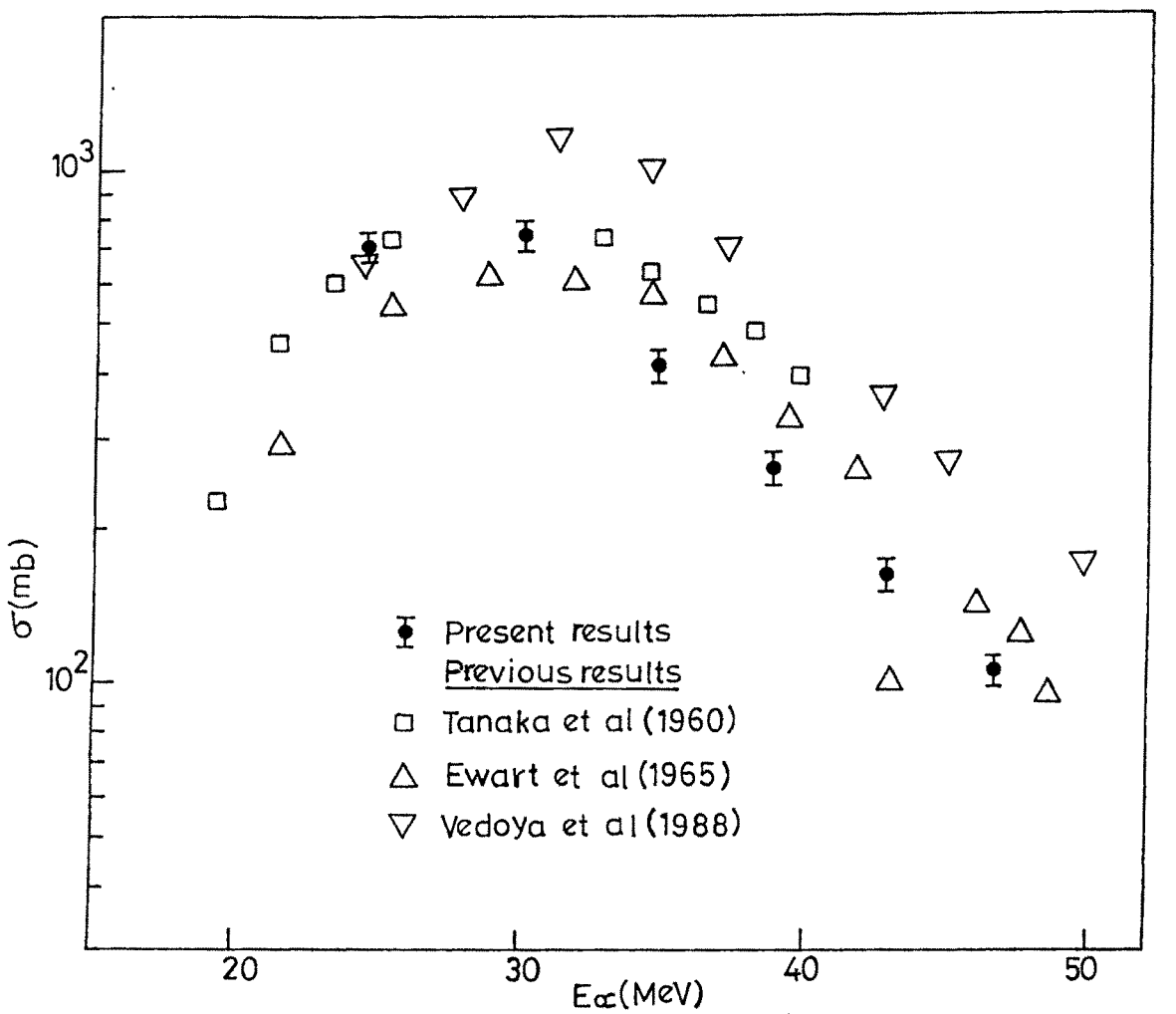

Fig.IV.23 EXCITATION FUNCTION OF $^{56}Fe(\alpha,Pn)^{58}Co$ REACTION

present work we have reinvestigated this reaction using high resolution HPGe detector.

The product nucleus ^{58}Co has a meta stable state and ground state of half lives 9.15 h (spin 5^+) and 70.78 d (spin 2^+).The meta stable state decays to ground state through isomeric transition. In the present work, measurements were carried out after the short half life activity (i.e meta stable state) decayed in ground state. Hence we have measured total cross section. It is not clear from the previous results whether the reported cross section was total or merely ground state.

The product nucleus ^{58}Co was identified by its prominent 811 keV gamma ray. A typical gamma ray spectrum and partial decay scheme are shown in figure IV.26 and IV.27(c) respectively. It can be seen from figure IV.23 that the present results are more systematic and are in close proximity with those of Ewart et al. The reported values of Vedoya et al and Tanaka et al differ by more than 50% and 25% respectively.

IV.4.4 Excitation function of the ^{56}Fe(α, p2n)^{57}Co reaction :

This reaction also studied by all the three previous authors mentioned above. Tanaka et al /17/ measured the cross section with 122 and 136 keV gamma ray photo peaks using 1-3/4 inch diameter x 2 inch high well type scintillation counter. Ewart et al /18/ measured the γ-ray activity using 7.5 x 7.5 cm NaI(Tl) crystal with a 256 channel pulse height analyser. The uncertainty quoted in their measurement was less than 25%. Vedoya et al /19/ performed the measurement using 122 keV gamma ray and Ge spectroscopy system. However, there are disagreement among previous results . The cross sections measured by Ewart et al are lower by a factor of about 1.3 to that of Vedoya et al.

Secondly, the peculiarity with (α, p2n) and (α, 3n) reactions on the same target is that they produce isobaric residual nuclei, the one with higher Z being produced in the (α,3n) reaction. The isobar with higher Z decays to that of lower Z by β^+ emission and/or electron capture. Thus, since both these reactions are energetically possible (their threshold differ by couple of MeV), the cross section determined for lower Z isobar always include the contribution from higher Z isobar. It is precisely for this reason that Tanaka et al and Ewart et al measured cumulative cross sections. However Vedoya et al subtracted contribution of (α,3n) reaction from (α,p2n) reaction.

In the present work we have made reinvestigation of this reaction exclusively and carefully using complex cross section formula of chapter III 3.6 eqn.(13) by which the contribution of (α,3n) reaction subtracted from (α,p2n) reaction. The product nuclei ^{57}Co having half life 271.6 days and spin $7/2^-$, was identified by its characteristic 122 and 136 keV gamma rays. A typical gamma ray spectrum and partial decay scheme are shown in figure IV.26 and IV.27(d) respectively. The cross sections were calculated using 122 keV gamma ray with an error less than 7%. It can be seen from figure IV.24 that our results are in close agreement with Tanaka et al and Vedoya et al where as result of Ewart et al differ by a factor of 1.5

IV.4.5 Excitation function of the ^{56}Fe(α,p3n)^{56}Co reaction:

As pointed out previously, the study of (α,pxn) reactions by activation technique, as far as the excitation function is concerned, are generally complicated by the possibility of isobaric precursor coming from (α.xn) reactions. In the present case the interfering contribution in the measurement of (α,p3n) cross section is

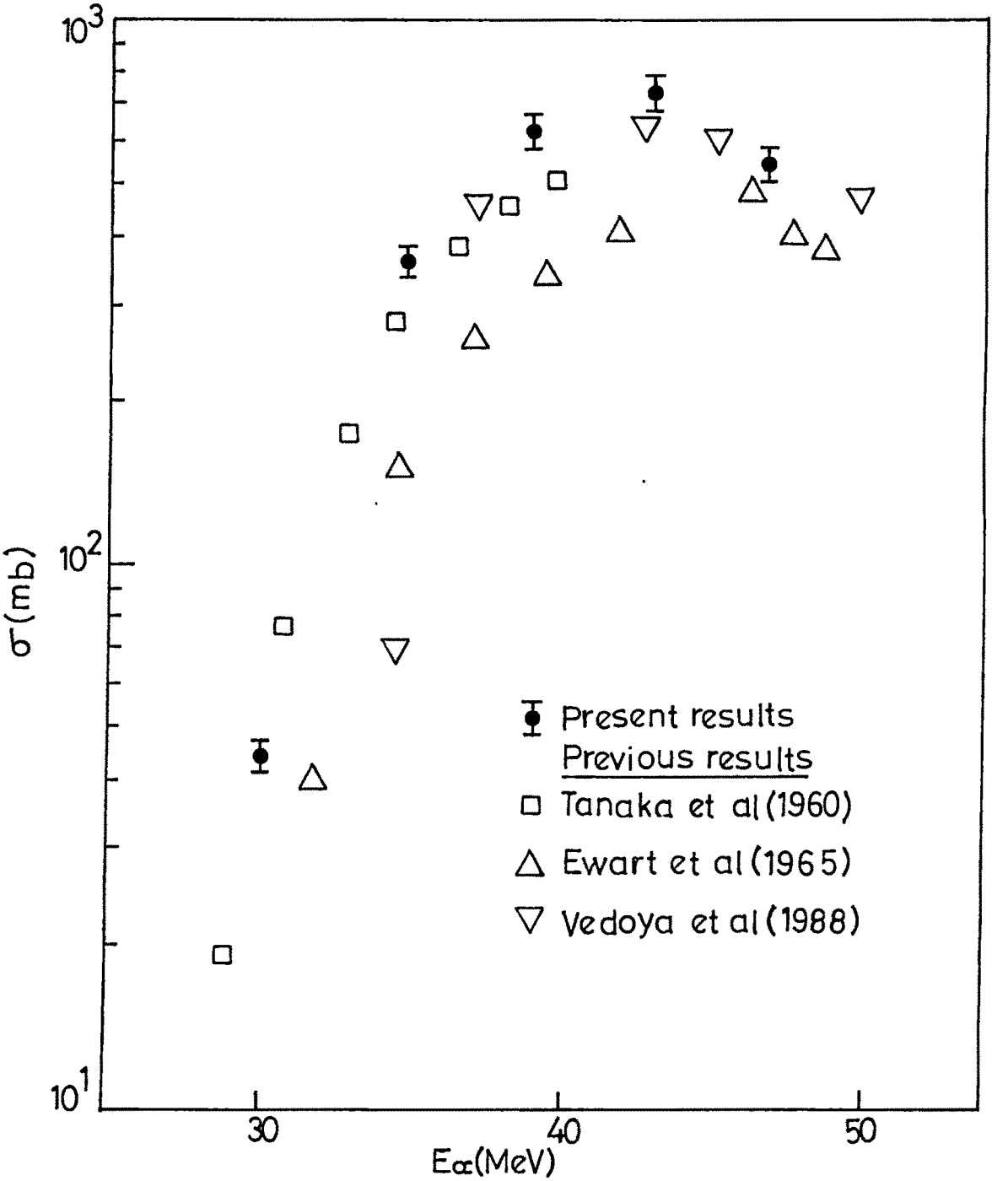

Fig.IV.24 EXCITATION FUNCTION OF $^{56}Fe(\alpha,p2n)^{57}Co$ REACTION

coming from (α,4n) reaction. In such case, cross sections of (α,p3n) reaction are exclusively calculated using the eqn.(13) of chapter III.3.6 .

The product nucleus ^{56}Co having half life 78.76 d and spin 4^+ was identified by its characteristic 847 and 1238 keV gamma rays. A typical gamma ray spectrum and partial decay scheme are shown in figure IV.26 and IV.27(e) respectively. The cross section measurement was done using 847 keV gamma ray as shown in figure IV.25 together with previous results /18,19/. It can be seen from figure that due to rather large threshold energy for this reaction and limited energy of α-particles, only a few energy points in the initial rising part of the experimental excitation function were studied.

A complete summary of the results obtained in the present experimental study is given in the table IV.4.

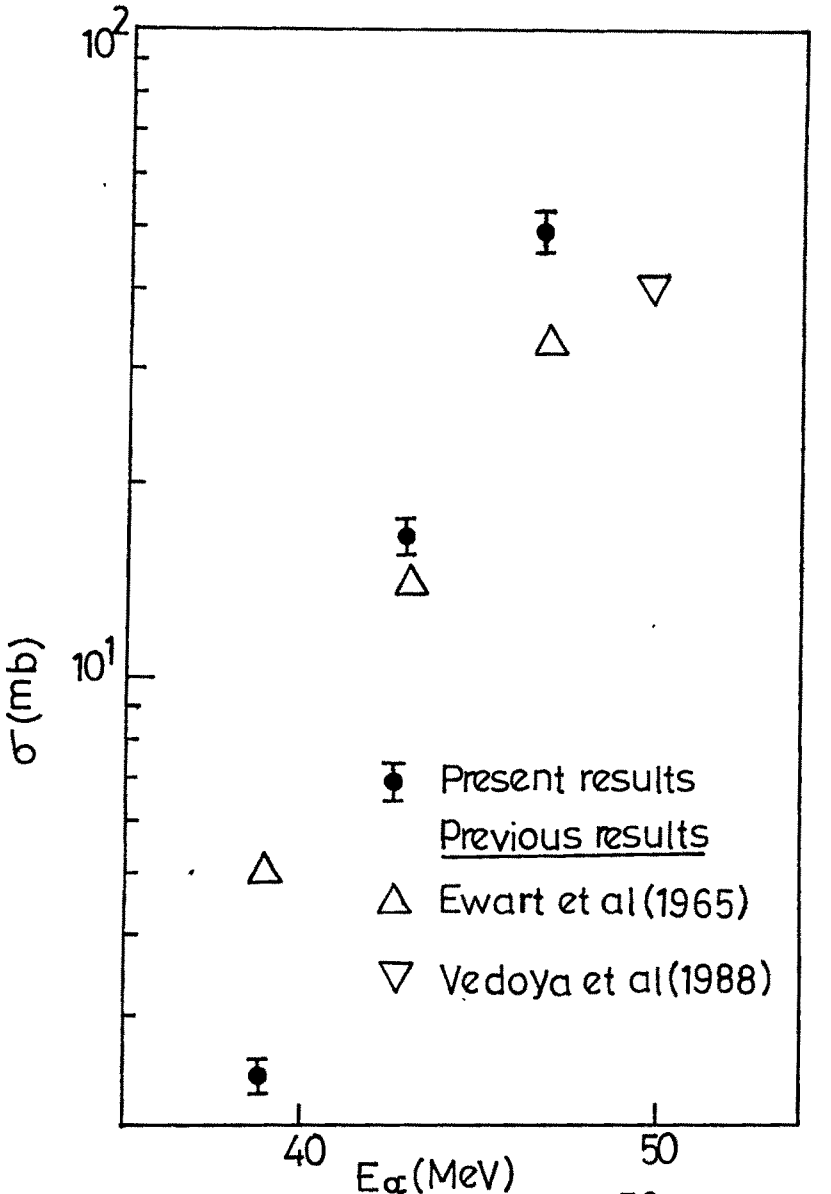

Fig. IV.25 EXCITATION FUNCTION OF $^{56}Fe(\alpha, p3n)^{56}Co$ REACTION

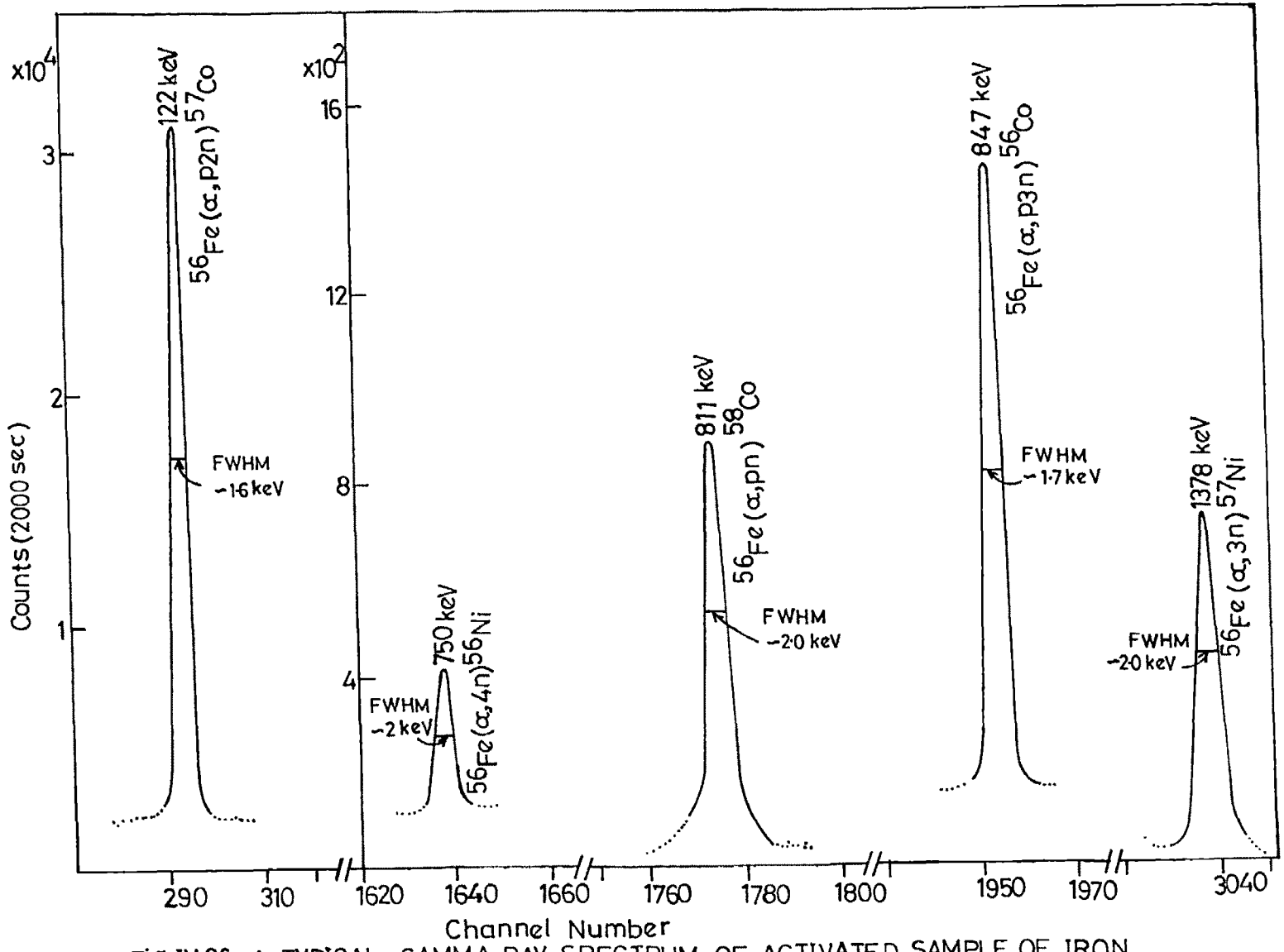

Fig.IV.26 A TYPICAL GAMMA RAY SPECTRUM OF ACTIVATED SAMPLE OF IRON

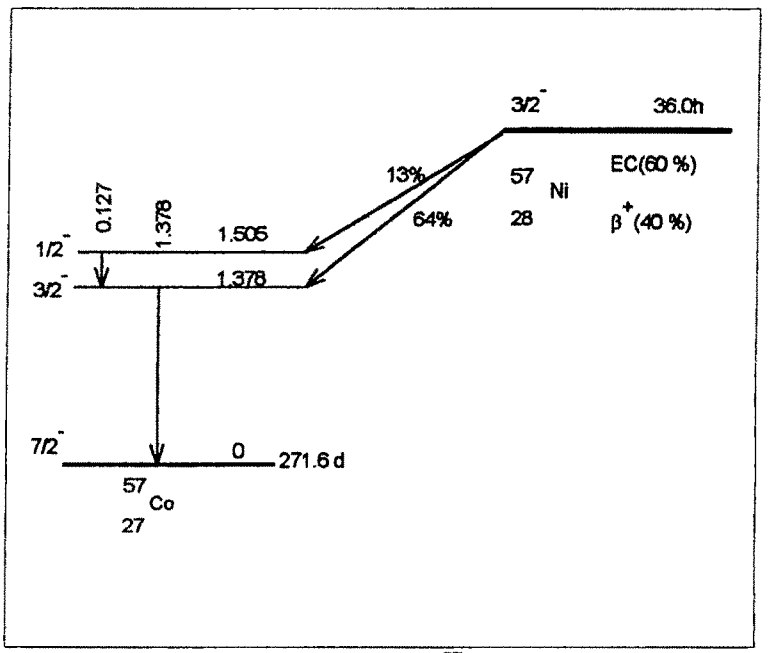

Fig.IV.27(a) Partial decay scheme of ^{57}Ni

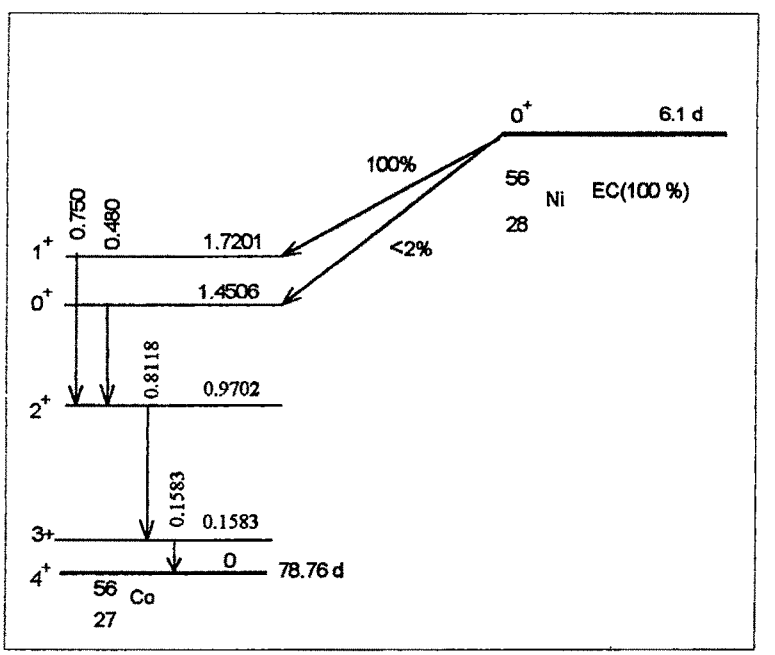

Fig.IV.27(b) Partial decay scheme of ^{56}Ni

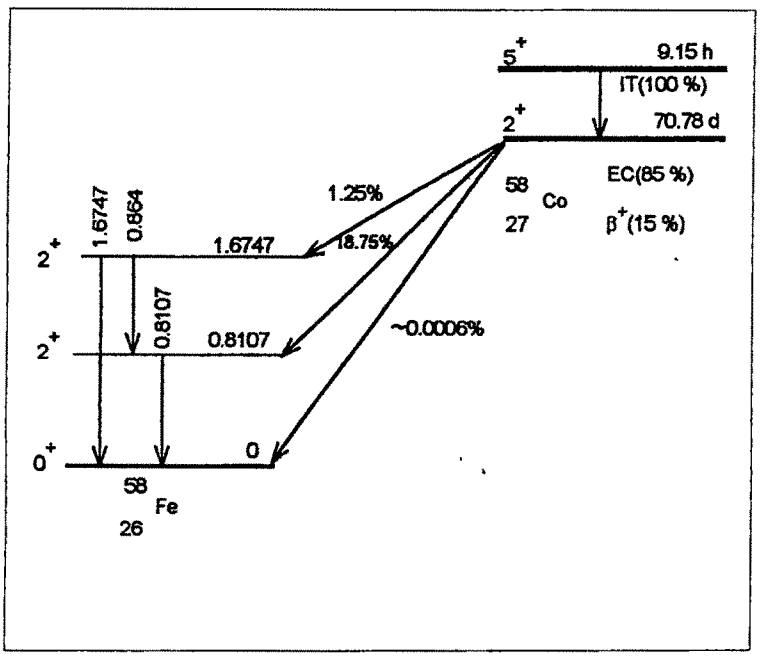

Fig.IV.27(c) Partial decay scheme of ^{58}Co

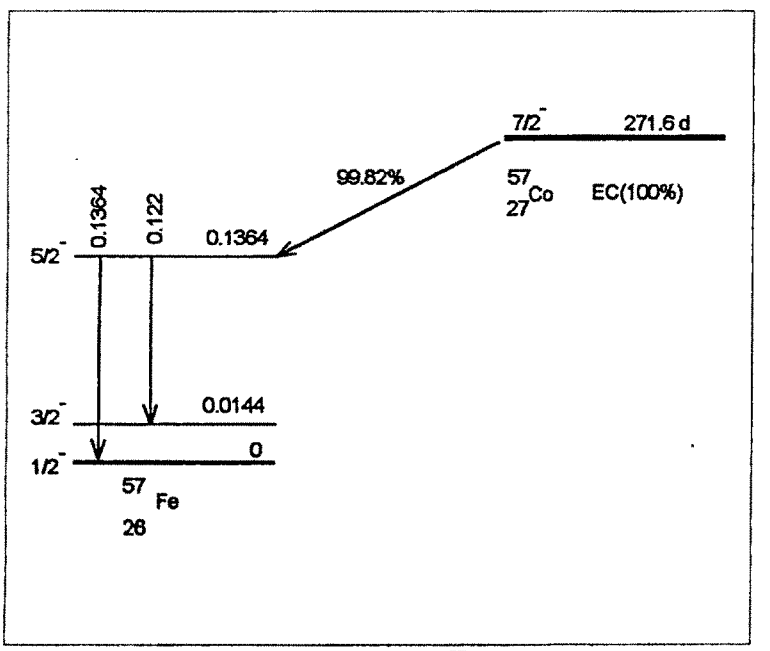

Fig.IV.27(d) Partial decay scheme of ^{57}Co

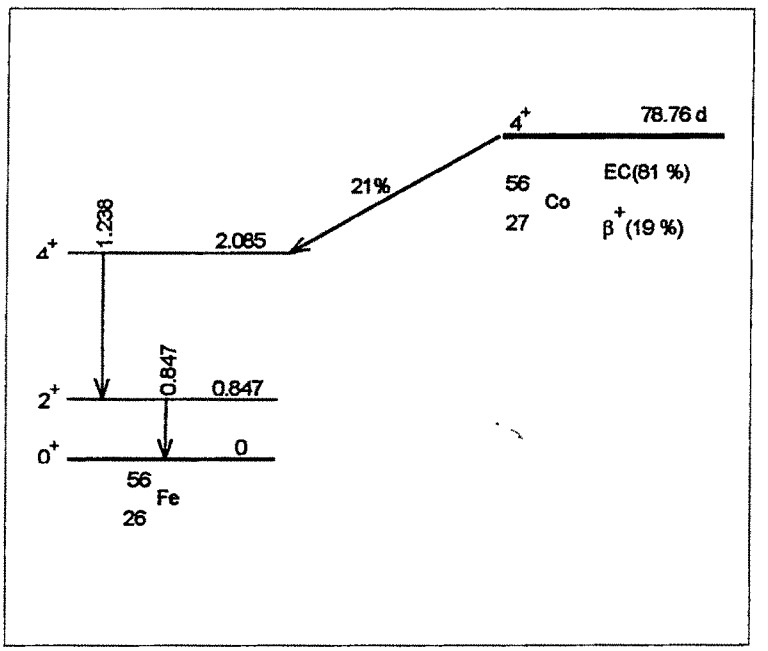

Fig.IV.27(e) Partial decay scheme of ^{56}Co

Table IV.4 Cross sections of the α-induced reaction on ^{56}Fe measured in the present work.

Reaction	**$^{56}Fe(\alpha,3n)$**	**$^{56}Fe(\alpha,4n)$**	**$^{56}Fe(\alpha,pn)$**	**$^{56}Fe(\alpha,p2n)$**	**$^{56}Fe(\alpha,p3n)$**
Product nucleus	**^{57}Ni**	**^{56}Ni**	**$^{58m+g}Co$**	**^{57}Co**	**^{56}Co**
Threshold energy (MeV)	**28.20**	**39.17**	**14.68**	**23.86**	**36.04**
E_α(MeV)	**σ(mb)**	**σ(mb)**	**σ(mb)**	**σ(mb)**	**σ(mb)**
24.5			705.0±51.7		
30.0	01.0±0.06		740.2±54.0	044.0±03.0	
34.7	04.4±0.30		409.2±30.0	357.1±24.5	
38.9	09.9±0.70		261.0±17.9	622.9±45.7	02.4±0.2
42.9	16.3±1.20	3.0±0.2	161.9±11.1	734.2±53.9	16.5±1.1
46.7	18.9±1.40	9.9±0.6	104.7±07.2	536.3±39.4	48.9±3.3

References :

/1/ D.J.Shah, H.B.Patel, N.L.Singh, S.Mukherjee and S.N.Chintalapudi, Pramana J. Phys. **44**,535(1995).

/2/ F.M.Lanzafame and M. Blann , Nucl.Phys. **A142**, 545 (1970).

/3/ H.E.Kurz, E.W. Jasper, K.Fischer and F. Hermes, Nucl.Phys. **A168**, 129 (1971).

/4/ O.A.Capurro, M. De.La. Vega Vedoya, C.Wasilevsky and S.J. Nassif, J.Radioanal Nucl. Chem. **89/2**, 519(1985).

/5/ H.D.Bhardwaj and R.Prasad , Nucl.Inst. & Meth. **A242**, 286 (1986).

/6/ P.Misaelides and H.Muenzel, J.Inorg. Nucl. Chem. **42**, 937(1980)

/7/ N.L.Singh, D.J.Shah, S.Mukherjee and S.N.Chintalapudi , Il Nuovo Cimento **A110**, 693(1997).

/8/ A.Calboreanu, C.Pencea and O. Salagean , Nucl.Phys. **A383**, 251 (1982) .

/9/ M. Ismail, Pramana J.Phys. **32**, 605(1989).

/10/ B.P.Singh, H.P.Bhardwaj and R.Prasad, Can. J. Phys. **69**, 1376 (1991).

/11/ M.K. Bhardwaj, I.A.Rizvi and A.K.Chaubey, Int.J. Mod.Phys. **E3**, 239 (1994).

/12/ D.J.Shah and N.L.Singh, Acta Physica Slovaca **47**,465(1997).

/13/ L.F. Hansen and M.I.Stelts, Phys.Rev. **136**, 1000 (1964).

/14/ M. K. Bhardwaj, I.A. Rizvi and A.K. Chaubey, Int. J. Mod. Phys. **E 3** , 389 (1992).

/15/ S.Mukherjee, M.H.Rashid and S.N.Chintalapudi, Indian J.Phys. **69A**, 455(1995).

/16/ N.L.Singh,D.J.Shah and H.B.Patel, Can.J.Phys. **76**, 785 (1998).

/17/ S. Tanaka, M. Furukawa, S.Iwata, Mauso, Yagi, Amano and Mikumo, J. Phys. Soc. Japan **15**, 2125 (1960).

/18/ A. Ewart , C. Valentine and M. Blann , Nucl.Phys. **69**, 625 (1965).

/19/ M. De. La. Vega Vedoya, O. Capurro, A.Archenti and S.J. Nassiff, J. Radioanal and Nucl.Chem. Articles **120**, 49 (1988).